(12) INTERNATIONAL APPLICATION PUBLISHED UNDER THE PATENT COOPERATION TREATY (PCT)

(19) World Intellectual Property Organization
International Bureau

(43) International Publication Date
22 May 2020 (22.05.2020)

WIPO | PCT

(10) International Publication Number
WO 2020/099487 A1

(51) International Patent Classification:
G01N 33/68 (2006.01)

(21) International Application Number:
PCT/EP2019/081177

(22) International Filing Date:
13 November 2019 (13.11.2019)

(25) Filing Language: English

(26) Publication Language: English

(30) Priority Data:
18206142.4 14 November 2018 (14.11.2018) EP
19189109.2 30 July 2019 (30.07.2019) EP

(71) Applicant: **VRIJE UNIVERSITEIT BRUSSEL** [BE/BE]; Pleinlaan 2, 1050 Brussel (BE).

(72) Inventors: **VAN GRUNSVEN, Leo**; Faculty of Medicine & Pharmacy, Laarbeeklaan 103, 1090 Jette (BE). **LAMBRECHT, Joeri**; Rue des deux ponts 29, 7850 Marcq (Enghien) (BE).

(74) Agent: **LC PATENTS**; Kempische Steenweg 542A, 3500 Hasselt (BE).

(81) Designated States *(unless otherwise indicated, for every kind of national protection available)*: AE, AG, AL, AM, AO, AT, AU, AZ, BA, BB, BG, BH, BN, BR, BW, BY, BZ, CA, CH, CL, CN, CO, CR, CU, CZ, DE, DJ, DK, DM, DO, DZ, EC, EE, EG, ES, FI, GB, GD, GE, GH, GM, GT, HN, HR, HU, ID, IL, IN, IR, IS, JO, JP, KE, KG, KH, KN, KP, KR, KW, KZ, LA, LC, LK, LR, LS, LU, LY, MA, MD, ME, MG, MK, MN, MW, MX, MY, MZ, NA, NG, NI, NO, NZ, OM, PA, PE, PG, PH, PL, PT, QA, RO, RS, RU, RW, SA, SC, SD, SE, SG, SK, SL, SM, ST, SV, SY, TH, TJ, TM, TN, TR, TT, TZ, UA, UG, US, UZ, VC, VN, ZA, ZM, ZW.

(84) Designated States *(unless otherwise indicated, for every kind of regional protection available)*: ARIPO (BW, GH, GM, KE, LR, LS, MW, MZ, NA, RW, SD, SL, ST, SZ, TZ, UG, ZM, ZW), Eurasian (AM, AZ, BY, KG, KZ, RU, TJ, TM), European (AL, AT, BE, BG, CH, CY, CZ, DE, DK, EE, ES, FI, FR, GB, GR, HR, HU, IE, IS, IT, LT, LU, LV, MC, MK, MT, NL, NO, PL, PT, RO, RS, SE, SI, SK, SM, TR), OAPI (BF, BJ, CF, CG, CI, CM, GA, GN, GQ, GW, KM, ML, MR, NE, SN, TD, TG).

Declarations under Rule 4.17:
— *as to applicant's entitlement to apply for and be granted a patent (Rule 4.17(ii))*
— *as to the applicant's entitlement to claim the priority of the earlier application (Rule 4.17(iii))*
— *of inventorship (Rule 4.17(iv))*

Published:
— *with international search report (Art. 21(3))*
— *with sequence listing part of description (Rule 5.2(a))*

(54) Title: SOLUBLE PDGFRBETA AS A BIOMARKER FOR FIBROSIS

(57) Abstract: The present application relates to the use of platelet derived growth factor β (PDGFRβ) as a biomarker for fibrosis. More specifically, the invention is directed to *in vitro* methods of diagnosing fibrosis, diagnosing the severity of fibrosis, determining the prognosis of fibrosis and/or assessing the efficacy of a therapeutic against fibrosis based on the detection and quantification of soluble PDGFRβ (sPDGFRβ) in biological fluid samples. Even more in particular, sPDGFRβ is determined for the diagnosis of liver fibrosis, lung fibrosis or kidney fibrosis. In another further aspect, the detection of sPDGFRβ is combined with the detection and/or quantification of other biomarkers. In a further embodiment detection and quantification of sPDGFRβ is combined with one or more other biomarkers.

WO 2020/099487 A1

Soluble PDGFRbeta as a biomarker for fibrosis

FIELD OF THE INVENTION

The present application relates to the use of platelet derived growth factor beta (PDGFRβ) as a biomarker for fibrosis. More specifically, the invention is directed to *in vitro* methods of diagnosing fibrosis, diagnosing the severity of fibrosis, determining the prognosis of fibrosis and/or assessing the efficacy of a therapeutic against fibrosis based on the detection and quantification of soluble PDGFRβ (sPDGFRβ) in biological fluid samples. Even more in particular, sPDGFRβ is determined for the diagnosis of liver fibrosis, lung fibrosis or kidney fibrosis. In another further aspect, the detection of sPDGFRβ is combined with the detection and/or quantification of one or more other biomarkers. In a further embodiment detection and quantification of sPDGFRβ is combined with one or more other biomarkers, such as albumin level, thrombocyte levels or circulating miRNAs.

BACKGROUND TO THE INVENTION

Fibrosis, or the net accumulation of extracellular matrix or scar can occur at different sites of the human body, including the lungs, liver or kidney. Diagnosis of fibrosis onset and regression remains a controversial subject in the current clinical setting, as the gold standard remains the invasive local biopsy, which is associated with multiple drawbacks.

For example, diagnosis of liver fibrosis onset and progression remains an important issue in the current clinical settings. The gold standard, and the diagnostic tool with the highest specificity and sensitivity, remains the liver biopsy, an invasive procedure associated with multiple drawbacks including inter- and intra-observer variability, discomfort for the patient and a doubtable cost-benefit ratio. In order to overcome these drawbacks, multiple non-invasive diagnostic tools have been proposed. Imaging modalities are a subgroup of such non-invasive diagnostic tools, measuring the elastic properties and stiffness of the liver tissue. Transient elastography (Fibroscan), acoustic radiation force impulse (ARFI), and magnetic resonance elastography (MRE) are some examples which have been validated in various etiologies of liver disease. Furthermore, the use of serological markers has been proposed for non-invasive assessment of liver fibrosis. The use of such serum markers may rely on the detection of a single parameter, or a group of parameters combined into a diagnostic algorithm. In the current clinical setting, several serological algorithms have gained popularity, such as the fibrosis 4 (Fib-4) score, enhanced liver fibrosis (ELF) test, aspartate aminotransferase/alanine aminotransferase (AST/ALT) ratio, and the AST to platelet ratio index (APRI). However, although the implementation of serological markers and imaging modalities has led to a reduced use of invasive liver biopsy, it has not yet led to its full redundancy. Such redundancy can only be obtained when a non-invasive marker has been found which is independent of liver disease etiology, easily accessible, with low cost, and with high specificity and sensitivity for both early

and late stages of liver fibrosis. Especially, the limited accuracy for diagnosis of onset and progression of early stage liver fibrosis remains a drawback of current non-invasive diagnostic tools, which thus prevents an as early as possible therapeutic intervention or life style change to avoid fibrosis progression.

MicroRNAs (miRNAs) are non-coding, single-stranded RNA structures of approximately 22 nucleotides long, and function as posttranscriptional gene regulators. More specific, through binding to the 3' untranslated regions of target messenger RNAs (mRNA), they can induce their cleavage, or prevent their translation into protein. Some miRNAs are known to be expressed in a cell- or tissue-specific manner. miRNAs are found in almost all body fluids, where they obtain stability by packaging into extracellular vesicles, or association to Argonaute2 or high-density lipoproteins. Recent research has identified the potential of miRNAs to be used as diagnostic tools for specific subsets of liver disease, often focusing on the diagnosis of liver cirrhosis and hepatocellular carcinoma (HCC). However, the diagnostic value of individual miRNAs, or miRNA-panels or miRNA in combination with other biomarkers, for the identification of early stages of liver fibrosis in heterogeneous patient populations remains to be proven.

In the search for novel non-invasive biomarkers, the inventors of the present application have found that soluble PDGFRβ, whether or not in combination with other biomarkers, can be used as a diagnostic agent for fibrosis, in particular liver fibrosis. PDGFRβ is one variant of PDGFR and its expression increases during activation of hepatic stellate cells (HSCs). Due to its dynamic expression and strong pro-mitogenic character, focus has been put on PDGFRβ as a therapeutic target in various basic and clinical studies using inhibitors of receptor tyrosine kinases, anti-PDGFRβ macromolecules, and cyclic peptide analogues of PDGF-BB, often leading to a significant inhibition of HSC activation and subsequent improvement of the liver condition. Despite its interest as a therapeutic target, not much was known concerning its use as diagnostic agent.

SUMMARY OF THE INVENTION

The present invention relates to the use of soluble platelet derived growth factor β (sPDGFRβ) as a biomarker for the diagnosis of fibrosis, in particular liver fibrosis, lung fibrosis or kidney fibrosis; preferably liver fibrosis.

In a first aspect, the invention discloses an *in vitro* method of diagnosing fibrosis in a subject, said method comprising: a) determining the level of soluble PDGFRβ (sPDGFRβ) in a biological fluid test sample obtained from said subject; and b) comparing said level of sPDGFRβ to a reference level of sPDGFRβ that is characteristic of a healthy subject without fibrosis in order to diagnose whether the subject has fibrosis, wherein an increase in sPDGFRβ in the test sample

compared to the reference level is indicative for fibrosis.

In another aspect, the invention discloses an *in vitro* method of diagnosing the severity of fibrosis in a subject. Said method comprises a) determining the level of sPDGFRβ in a biological fluid test sample obtained from said subject, and b) comparing said level of sPDGFRβ to a predetermined level of said sPDGFRβ in a population of subjects ranging from no fibrosis to severe fibrosis.

In yet another aspect, the invention discloses an *in vitro* method of determining the prognosis of fibrosis in a subject, said method comprising: a) determining the level of sPDGFRβ in a biological fluid test sample obtained from said subject, and b) comparing said level of sPDGFRβ to a reference level of sPDGFRβ that is characteristic of a healthy subject without fibrosis in order to determine the prognosis of fibrosis in said subject, wherein an increase in sPDGFRβ in the test sample compared to the reference level is indicative for the prognosis of the subject.

In a further aspect, the invention discloses an *in vitro* method of assessing the efficacy of a therapeutic agent against fibrosis in a subject, said method comprising a) determining the level of sPDGFRβ in a first biological fluid test sample obtained from said subject wherein said first biological fluid test sample is obtained at a time point before the start of treatment, b) determining the level of sPDGFRβ in one or more subsequent biological fluid test samples obtained from said subject wherein said one or more subsequent biological test samples are obtained at regular intervals after the start of the treatment, c) comparing the level of sPDGFRβ in the first biological fluid test sample with the level of sPDGFRβ in the one or more subsequent biological fluid test samples in order to assess the efficacy of the therapeutic agent. In said method, a decrease in the level of sPDGFRβ in the one or more subsequent test samples as compared to the level of sPDGFRβ in the first test sample is indicative for a decrease in disease progression in the subject. Also in said method, an increase in the level of sPDGFRβ in the one or more subsequent test samples as compared to the level of sPDGFRβ in the first test sample is indicative for an increase in diseases progression in the subject.

In accordance with each of the foregoing aspects and embodiments, the *in vitro* methods according to the different aspects of the invention can be combined with the analysis of the level(s) of one or more additional biomarkers for fibrosis. Therefore, the *in vitro* methods according to the different aspects of the invention are further characterized in that the biological fluid test sample is further analysed to determine the level(s) of one or more additional biomarkers for fibrosis, and wherein the level(s) of said one or more additional biomarkers are compared to the reference levels of said one or more additional biomarkers that are characteristic of a healthy subject without fibrosis in order to diagnose the presence of severity

of fibrosis or in order to determine the prognosis of fibrosis in said subject.

In a further aspect, the one or more additional biomarkers are selected from the group comprising aspartate transaminase (AST), alanine transaminase (ALT), alkaline phosphatase, bilirubin, albumin, gamma-glutamyl transferase, creatinine, alpha-fetoprotein, the thrombocyte level and the level of one or more circulating miRNAs. In a further aspect, the one or more additional biomarkers are albumin and the thrombocyte level. In another further aspect, the one or more additional biomarkers are at least one miRNA; preferably at least five circulating miRNAs.

In one of the aspects of the invention, in the *in vitro* methods according to the different aspects of the invention the determination of sPDGFRβ levels can further be combined with the analysis of the levels of circulating miRNAs in the subject. In a further embodiment, in the *in vitro* methods of diagnosing fibrosis, diagnosing the severity of fibrosis or determining the prognosis of fibrosis in a subject the determination of sPDGFRβ levels in the subject is further combined with determining the level of at least one circulating miRNA in the subject; preferably at least five circulating miRNAs in the subject. In a further embodiment, said circulating miRNAs are selected from miRNA-451a, miRNA-142-5p, Let-7f-5p, miRNA-378-3p, miRNA-122-5p, and miRNA-29a-3p; even more preferably selected from miRNA-451a, miRNA-142-5p, Let-7f-5p, miRNA-122-5p and miRNA-29a-3p.

In an even further aspect, in the *in vitro* methods of diagnosing fibrosis, diagnosing the severity of fibrosis or determining the prognosis of fibrosis in a subject, the determined sPDGFRβ levels are further combined with calculating the miRFIB score, wherein the miRFIB score is calculated using the following formula: miRFIB score = 4.3799 + (0.70824 x Let-7f-5p (dCT)) – (0.090912 x miRNA-122-5-p (dCT)) – (0.26149 x miRNA-142-5p (dCT)) – (0.53602 x miRNA-29a-3p (dCT)) – (0.041140 x miRNA-451a (dCT)), wherein dCT represents the delta CT value of each specific miRNA determined using real-time PCR.

In a further preferred aspect, the present invention discloses an *in vitro* method of diagnosing the presence and/or severity of fibrosis, preferably liver fibrosis, in a subject, wherein said method comprises calculating the PRTA score ("s**P**DGF**R**β-**T**hrombocyte-**A**lbumin" score), and comparing the PRTA score of said subject to the PRTA score of a healthy subject without fibrosis, wherein the PRTA score is calculated using the formula: [sPDGFRβ (pg/mL) *100]/ [albumin (g/L) * (thrombocytes (/mm^3)/100)], and wherein the levels of sPDGFRβ, albumin and thrombocytes are determined in a biological fluid test sample obtained from the subject.

The invention is further directed to an *in vitro* method of determining the prognosis of fibrosis; preferably liver fibrosis, in a subject, said method comprising: calculating the PRTA score, and comparing the PRTA score of said subject to the PRTA score of a healthy subject without

fibrosis, wherein the levels of sPDGFRβ, albumin and thrombocytes are determined in a biological fluid test sample obtained from the subject. In said method, an increase in the PRTA score in the test sample compared to the reference sample is indicative for the prognosis of the subject.

In another embodiment, the invention is directed to an *in vitro* method of assessing the efficacy of a therapeutic agent against fibrosis; preferably liver fibrosis, in a subject, said method comprising: a) calculating the PRTA score of said subject at a first time point before the start of the treatment, b) calculating the PRTA score of said subject at one or more second time points at regular intervals after the start of the treatment, c) comparing the PRTA score of the first time point with the PRTA score of the one or more second time points in order to assess the efficacy of the therapeutic agent, wherein the levels of sPDGFRβ, albumin and thrombocytes are determined in a biological fluid test sample obtained from the subject. A decrease of the PRTA score of the one or more second time points as compared to the PRTA score of the first time point is indicative for a decrease in disease progression in the subject, whereas an increase of the PRTA score of the one or more second time points as compared to the PRTA score of the first time point is indicative for an increase in disease progression in the subject.

In all the different embodiments of the present invention, the PRTA score is calculated using the formula: [sPDGFRβ (pg/mL) *100]/ [albumin (g/L) * (thrombocytes (/mm^3)/100)].

In one of the aspects of the invention, and in the *in vitro* methods according to the different embodiments, the determination of PRTA score can further be combined with the analysis of the levels of circulating miRNAs in the subject. In a further embodiment, in the *in vitro* methods of diagnosing fibrosis, diagnosing the severity of fibrosis or determining the prognosis of fibrosis in a subject the determination of the PRTA score in the subject is further combined with determining the level of at least one circulating miRNA in the subject; preferably at least five circulating miRNAs in the subject. In a further embodiment, said circulating miRNAs are selected from miRNA-451a, miRNA-142-5p, Let-7f-5p, miRNA-378-3p, miRNA-122-5p, and miRNA-29a-3p; even more preferably selected from miRNA-451a, miRNA-142-5p, Let-7f-5p, miRNA-122-5p and miRNA-29a-3p.

In an even further aspect, in the *in vitro* methods of diagnosing fibrosis, diagnosing the severity of fibrosis or determining the prognosis of fibrosis in a subject, the determined PRTA score is further combined with calculating the miRFIB score, wherein the miRFIB score is calculated using the following formula: miRFIB score = 4.3799 + (0.70824 x Let-7f-5p (dCT)) – (0.090912 x miRNA-122-5-p (dCT)) – (0.26149 x miRNA-142-5p (dCT)) – (0.53602 x miRNA-29a-3p (dCT)) – (0.041140 x miRNA-451a (dCT)), wherein dCT represents the delta CT value of each specific miRNA determined using real-time PCR. The PRTA score is calculated as disclosed herein

above.

In still a further aspect, the present invention provides an *in vitro* method of diagnosing the presence and/or severity of fibrosis; preferably liver fibrosis, in a subject, said method comprising calculating the miRFIB^p score and comparing the miRFIB^p score of said subject to the miRFIB^p score of a healthy subject without fibrosis, wherein the miRFIB^p score is calculated using the formula: miRFIB^p-score = (0.97229 x miRFIBscore) + (0.00021150 x PDGFRβ (pg/ml)) - 1.8678, wherein the miRFIB score is calculated as disclosed herein above, and wherein the levels of sPDGFRβ and circulating miRNAs are determined in a biological fluid test sample obtained from the subject.

In still another aspect, the present invention provides an *in vitro* method of determining the prognosis of fibrosis; preferably liver fibrosis, in a subject, said method comprising calculating the miRFIB^p score and comparing the miRFIB^p score of said subject to the miRFIB^p score of a healthy subject without fibrosis, wherein the miRFIB^p score is calculated using the formula: miRFIB^p-score = (0.97229 x miRFIBscore) + (0.00021150 x PDGFRβ (pg/ml)) - 1.8678, wherein the miRFIB score is calculated as disclosed herein above, wherein the levels of sPDGFRβ and circulating miRNAs are determined in a biological fluid test sample obtained from the subject, and wherein an increase in the miRFIB^p-score in the biological fluid test sample compared to the reference level is indicative for the prognosis of the subject.

In another aspect, the present invention provides an *in vitro* method of assessing the efficacy of a therapeutic agent against fibrosis, preferably against liver fibrosis, in a subject, said method comprising:

a) calculating the miRFIB^p score of said subject at a first time point before the start of the treatment,

b) calculating the miRFIB^p score of said subject at one or more second time points at regular intervals after the start of the treatment,

c) comparing the miRFIB^p score of the first time point with the miRFIB^p score of the one or more second time points in order to assess the efficacy of the therapeutic agent, wherein the miRFIB^p score is calculated as disclosed herein above, and wherein the levels of sPDGFRβ and circulating miRNAs are determined in a biological fluid test sample obtained from the subject, and wherein a decrease in the miRFIB^p score of the one or more second time points as compared to the miRFIB^p score of the first time point is indicative for a decrease in disease progression in the subject, and wherein an increase of the miRFIB^p score of the one or more second time points as compared to the miRFIB^p score of the first time point is indicative for an increase in disease progression in the subject.

Further, all the *in vitro* methods according to the different embodiments of the invention are directed to the detection and/or quantification of sPDGFRβ and optionally one or more additional biomarkers, or the miRFIB score or the miRFIB^{p} score for assessing the diagnosis, prognosis and/or therapy efficacy of fibrosis. In a further embodiment, fibrosis can be lung fibrosis, liver fibrosis or kidney fibrosis; preferably liver fibrosis. In an even more preferred embodiment, the *in vitro* methods according to all the different embodiments of the invention are directed to the detection and/or quantification of sPDGFRβ and optionally one or more additional biomarkers for assessing the diagnosis, prognosis and/or therapy efficacy of liver fibrosis.

In another aspect, the present application is directed to an *in vitro* method of diagnosing the presence and/or severity of fibrosis, preferably liver fibrosis, in a subject, wherein said method comprises analysis of the levels of circulating miRNAs in the subject. In a further aspect, the in vitro method of diagnosing the presence and/or severity of fibrosis, preferably liver fibrosis, in a subject comprises analysis of the levels of at least one, preferably at least five circulating miRNAs in the subject. In still a further aspect, said circulating miRNAs are selected from miRNA-451a, miRNA-142-5p, Let-7f-5p, miRNA-378-3p, miRNA-122-5p, and miRNA-29a-3p; even more preferably selected from miRNA-451a, miRNA-142-5p, Let-7f-5p, miRNA-122-5p and miRNA-29a-3p.

In another aspect, the present application provides an in vitro method of diagnosing the presence and/or severity of fibrosis, preferably liver fibrosis, in a subject, wherein said method comprises calculating the miRFIB score, wherein the miRFIB score is calculated using the following formula: miRFIB score = 4.3799 + (0.70824 x Let-7F-5p (dCT)) – (0.090912 x miRNA-122-5-p (dCT)) – (0.26149 x miRNA-142-5p (dCT)) – (0.53602 x miRNA-29a-3p (dCT)) – (0.041140 x miRNA-451a (dCT)), wherein dCT represents the delta CT value of each specific miRNA determined using real-time PCR, and wherein said miRFIB score is compared to the miRFIB score of a healthy subject without fibrosis.

In yet another embodiment, the biological fluid sample according to all the different embodiments of the invention comprises blood, plasma, serum, saliva or urine. In a preferred embodiment, the biological fluid sample comprises blood, plasma or serum.

In still another embodiment, and in all the *in vitro* methods according to the different embodiments of the present invention, the levels of sPDGFRβ are determined using immuno-based technologies. In a further embodiment, said immuno-based technologies are selected from the group comprising enzyme-linked immunosorbent assay (ELISA), immune-chromatography, Luminex assays, CyTOF, immunofluorescence assays.

In still another embodiment, the levels of the one or more additional biomarkers are determined using immuno-based technologies. In a further embodiment, said immuno-based technologies are selected from the group comprising enzyme-linked immunosorbent assay (ELISA), immune-chromatography, Luminex assays, CyTOF, immunofluorescence assays. In still a further embodiment, the levels of aspartate transaminase (AST), alanine transaminase (ALT), alkaline phosphatase, bilirubin, albumin, gamma-glutamyl transferase, creatinine, and alpha-fetoprotein are determined using immuno-based technologies.

In another aspect, the levels of thrombocytes in the *in vitro* methods according to the different embodiments of the invention are determined using an automatic microscopy-based counting technology or an automated blood cell analyser.

In another embodiment of the present invention, the subject according to all the different embodiments of the invention is a human.

In another aspect, the present invention provides a method of treatment of a subject with fibrosis, in particular liver fibrosis, wherein said method comprises determining the level of sPDGFRβ in a biological fluid test sample obtained from said subject, and comparing said level of sPDGFRβ to a reference level of sPDGFRβ that is characteristics of a healthy subject without fibrosis in order to diagnose whether the subject has fibrosis, followed by administration of a therapeutic agent against fibrosis to the subject in order to treat the subject.

In another aspect, the present invention provides a method of treatment of a subject with fibrosis, in particular liver fibrosis, wherein said method comprises determining the level of sPDGFRβ in a first biological fluid test sample obtained from said subject wherein said first biological test sample is obtained at a time point before the start of the treatment, administering of a therapeutic agent against fibrosis to the subject, determining the level of sPDGFRβ in one or more subsequent biological fluid test samples obtained from said subject wherein said one or more subsequent biological test samples are obtained at regular intervals after the start of the treatment, and comparing the level of sPDGFRβ in the first biological fluid test sample with the level of sPDGFRβ in the one or more subsequent biological fluid test samples in order to assess the efficacy of the therapeutic agent.

In still another embodiment, the present invention provides a method of treatment of a subject with fibrosis, in particular liver fibrosis, wherein said method comprises calculating the PRTA score of a subject, wherein the PRTA score is calculated using the formula [sPDGFRβ (pg/mL) *100]/ [albumin (g/L) * (thrombocytes (/mm^3)/100)], and comparing said PRTA score to the PRTA score of a healthy subject without fibrosis in order to diagnose whether the subject has

fibrosis, followed by administration of a therapeutic agent against fibrosis in order to treat the subject.

In still another embodiment, the present invention provides a method of treatment of a subject with fibrosis, in particular liver fibrosis, wherein said method comprises calculating the miRFIB^p score and comparing said miRFIB^p score to the miRFIB^p score of a healthy subject without fibrosis in order to diagnose whether the subject has fibrosis, followed by administration of a therapeutic agent against fibrosis in order to treat the subject.

In yet another embodiment, the present invention provides a method of treatment of a subject with fibrosis, in particular liver fibrosis, wherein said method comprises calculating the PRTA score of said subject at a first time point before the start of the treatment, administering of a therapeutic agent against fibrosis to the subject, calculating the PRTA score of said subject at one or more second time points at regular intervals after the start of the treatment, and comparing the PRTA score of the first time point with the PRTA score of the one or more second time points in order to assess the efficacy of the therapeutic agent.

In yet another embodiment, the present invention provides a method of treatment of a subject with fibrosis, in particular liver fibrosis, wherein said method comprises calculating the miRFIB^p score of said subject at a first time point before the start of the treatment, administering of a therapeutic agent against fibrosis to the subject, calculating the miRFIB^p score of said subject at one or more second time points at regular intervals after the start of the treatment, and comparing the miRFIB^p score of the first time point with the miRFIB^p score of the one or more second time points in order to assess the efficacy of the therapeutic agent.

BRIEF DESCRIPTION OF THE DRAWINGS

With specific reference now to the figures, it is stressed that the particulars shown are by way of example and for purposes of illustrative discussion of the different embodiments of the present invention only. They are presented in the cause of providing what is believed to be the most useful and readily description of the principles and conceptual aspects of the invention. In this regard no attempt is made to show structural details of the invention in more detail than is necessary for a fundamental understanding of the invention. The description taken with the drawings making apparent to those skilled in the art how the several forms of the invention may be embodied in practice.

Fig. 1: PDGFRβ is enriched in HSC-derived extracellular vesicles (EVs). Differential centrifugation was used for purification of EVs from the culture medium of primary murine and human HSCs. **(A)** Nanoparticle tracking analysis was used to verify the size of purified EVs. **(B)**

Spontaneous activation of primary murine HSCs after plating on hard substrates allows the comparison of EVs derived from activated (aHSC, day 8 to 10 of culture) and quiescent HSCs (qHSC, day 0-2 of culture). WB analysis was performed on such purified EVs, using cell lysates of activated HSCs as control. Besides PDGFRβ analysis, the EV-purity was verified by presence of the EV-marker HSP70 and absence of the cellular marker calreticulin. **(C)** WB analysis was performed on EVs secreted by LX2s and activated primary human HSCs (hHSC), using their respective cell lysates as control. Protein expression of PDGFRβ and the EV-purity markers HSP70 and calreticulin was analyzed.

Figure 2: PDGFRβ expression is up-regulated in a CCl_4-induced mouse model of liver fibrosis. Mice were injected for 4 weeks, 2 times a week, with CCl_4 to induce liver injury. Mice were sacrificed 24 hours after the last CCl_4 injection. PDGFRβ-expression was found to be significantly up-regulated, as compared to non-treated mice of the same age, in total liver tissue of CCl_4-injected mice, both on **(A)** WB and **(B)** immune histochemical staining. **(A)** PDGFRβ and αSMA protein levels were quantified and normalized versus GAPDH expression (n = 5). Bars indicate the fold increase in CCl_4-induced mice compared to healthy controls. **(B)** The area of PDGFRβ positive staining was calculated by using image analysis software, and is plotted as percentage of the total area (n = 5). **(C)** PDGFRβ expression in the non-parenchymal fraction (NPF) and the different liver cell types, being Kupffer cells (KC), liver sinusoidal endothelial cells (LSEC), and hepatocytes, was analyzed by qPCR and compared to the RNA levels observed in quiescent HSCs. Error bars represent mean values ± SD.

Figure 3: Enhanced PDGFRβ expression in liver tissue of cirrhotic patients. Staining on total liver tissue of 3 healthy and 3 cirrhotic patients identified an enhanced collagen deposition (Sirius Red) and enhanced expression of PDGFRβ in cirrhotic patients only. The area of PDGFRβ-positive or Sirius Red-positive staining was calculated by using image analysis software, and is plotted as percentage of the total area. Error bars represent mean values ± SD.

Figure 4: Plasma sPDGFRβ expression in a heterogeneous patient population suffering from liver fibrosis/cirrhosis. (A) Plasma sPDGFRβ levels are progressively augmented with increasing fibrosis stage, and show the highest discriminative value for significant liver fibrosis (F ≥ 2). **(B)** The relationship between plasma sPDGFRβ levels and biochemical and metabolic parameters. **(C)** All three parameters of the PRTA score, being sPDGFRβ, albumin and thrombocytes, are significantly correlated with fibrosis progression. Error bars represent mean values ± SD. Correlation parameters were calculated with Spearman's correlations test.

Figure 5: Comparison of performance of sPDGFRβ, PRTA-score and Fib-4 in the diagnosis of liver fibrosis/cirrhosis. Receiver operating characteristic (ROC) curves for the non-invasive diagnosis of significant fibrosis (F ≥ 2), advanced fibrosis (F ≥ 3), and cirrhosis (F

= 4) comparing sPDGFRβ levels, the sPDGFRβ-containing PRTA-score, and the clinically used Fib-4 score.

Figure 6. miRNA expression in mouse in vitro activated hepatic stellate cells (HSCs). (**A**) mRNA expression levels determined by quantitative polymerase chain reaction (qPCR) of HSC-activation markers Acta2, Col1a1, and Lox in freshly isolated HSCs (0h), as compared to HSCs activated by 10 days of cultures (D10). (**B**) miRNA-451a, miRNA-142-5p, Let-7f-5p, and miRNA-378a-3p were found to be significantly dysregulated upon HSC activation. One-tailed unpaired t-test analysis was used to determine statistical significance. Results are shown as mean ± SEM; n = 5.

Figure 7. miRNA target prediction. Bioinformatics-based target prediction was carried out, using four different predictive algorithms: TargetScan, miRDB, starBase, and miRTarBase. (**A**) Venn diagram showing putative target genes for the differentially expressed miRNAs in culture activated primary mouse HSCs. A list of target genes mutual among all four miRNAs is shown. mRNA expression analysis of the identified mutual target genes in activated (D10) versus quiescent (0h) HSCs identified (**B**) three genes with no significant difference, (**C**) three genes to be significantly up-regulated and (D) seven genes to be significantly down-regulated. One-tailed unpaired t-test analysis was used to determine statistical significance. Results are shown as mean ± SEM; n = 5.

Figure 8. miRNA expression analysis in a CCl_4-induced mouse model of liver fibrosis. (**A**) Total liver tissue of mice that received CCl_4-injections two times a week, for a period of four weeks, and healthy controls, was used to visualize hepatocyte damage and inflammation (H&E), and cross-linked collagen deposition (Sirius Red). The area of Sirius Red positive staining was calculated, using Orbit analysis software and is plotted as percentage of the total area (n = 7 mice per group). (**B**) miRNA expression analysis of total liver tissue extracted from CCl_4-injected mice, as compared to healthy controls (n = 7 mice per group). Results are shown as mean ± SEM. (**C**) Tukey boxplots represent miRNA expression values in plasma obtained from CCl_4-injected mice, as compared to healthy controls (n = 7 mice per group). Obtained Ct levels were normalized by use of spiked-in Cel-miRNA-39. One-tailed unpaired t-test analysis was used to determine statistical significance.

Figure 9. miRNA expression analysis in liver cell types. miRNA expression levels were determined by use of qPCR and compared between hepatocytes, liver sinusoidal endothelial cells (LSEC), Kupffer cells (KC) and HSCs. Statistical significance was determined using one-way ANOVA with Dunnett's multiple comparison test. Results are shown as mean ± SEM; n = 6.

Figure 10. Evidence of significant liver fibrosis by plasma levels of individual miRNAs. Expression analysis of circulating miRNAs in patients (n = 208) with chronic alcohol abuse, viral infection, and NAFLD, with (F2-4) or without (F0-1) significant liver fibrosis. P-values were calculated using Mann-Whitney U-test. Data is presented as Tukey boxplots. Receiver operating characteristic curve analysis was performed, and AUC values were calculated to quantify diagnostic value. The discriminative capacity of (A) candidate miRNAs was compared to (B) miRNA-122-5p and (C) miRNA-29a-3p and to (D) the serological scoring algorithms Fib-4, APRI, AST/ALT, and PRTA.

Figure 11. Fibrosis-stage specific presence of circulating miRNAs. The total patient cohort was divided based on the elastography-proven stage of liver fibrosis. Significant differences in expression levels between the various stages of liver fibrosis were determined using the Kruskal-Wallis test with Dunn's multiple comparison test. Data is presented as Tukey boxplots.

Figure 12. Diagnostic performance of the miRFIB- and the miRFIBp-score for significant liver fibrosis. Performance comparison of the miRFIB-, the miRFIBp-score, and commonly used validated diagnostic algorithms for the diagnosis of significant liver fibrosis (F2-4) in (**A**) the derivation, (**B**) validation, and (**C**) total patient cohort.

DETAILED DESCRIPTION OF THE INVENTION

Definitions

In the context of the present application, "diagnosis" and "diagnosing" generally includes a determination of a subject's susceptibility to a disease or disorder, a determination as to whether a subject is presently affected by a disease or disorder, a prognosis of a subject affected by a disease or disorder, and therametrics (e.g., monitoring a subject's condition to provide information as to the effect or efficacy of therapy).

Also in the context of the present application, the terms "individual", "subject" and "patient" are used interchangeably herein, and they refer to any mammalian subject for whom diagnosis, treatment, or therapy is desired. In a preferred embodiment, the individual, subject or patient is a human. Other subject may include, but are not limited to, cattle, horses, dogs, cats, guinea pigs, rabbits, rats, primates, ducks, and mice.

The terms "prognosis" and "prognose" refer to the act or art of foretelling the course of a disease. Additionally, the terms refer to the prospect of survival and recovery from a disease as anticipated from the usual course of that disease or indicated by special features of the individual case. Further, the terms refer to the art or act of identifying a disease from its signs and symptoms.

The terms "treatment", "treating", "treat" and the like refer to obtaining a desired pharmacological and/or physiological effect. The effect may be prophylactic in terms of completely or partially

preventing a disease or symptom thereof and/or may be therapeutic in terms of a partial or complete stabilization or cure for a disease and/or adverse effect attributable to the disease. "Treatment" covers any treatment of a disease in a mammal, particularly a human, and includes: (a) preventing the disease or symptom form occurring in a subject which may be predisposed to the disease or symptom but has not yet been diagnosed as having it; (b) inhibiting the disease symptom, i.e. arresting its development; or (c) relieving the disease symptom, i.e. causing regression of the disease or symptom.

The term "biological fluid sample" encompasses a variety of fluid samples, including blood and other liquid samples of biological origin, obtained from an organism that may be used in a diagnostic or monitoring assay. The term specifically encompasses a clinical fluid sample, and further includes cell supernatants, cell lysates, serum, plasma, urine, amniotic fluid, biological fluids. The term also encompasses samples that have been manipulated in any way after procurement, such as treatment with reagents, solubilization, or enrichment for certain components.

"Fibrosis" refers to any of a variety of biological phenomena that are characteristic of a fibrotic cell. The phenomena can vary with the type of fibrosis, but the fibrosis phenotype is generally identified by abnormalities in scar tissue formation.

"Liver fibrosis" refers to any of a variety of biological phenomena that are characteristic of a fibrotic liver cell. Liver fibrosis can be divided in different forms, from mild fibrosis to severe fibrosis, which includes liver cirrhosis.

The term "reference level" as used in the context of this application refers to the level of a specific marker that is characteristic of a healthy subject which does not suffer of any type of fibrosis. It is further contemplated that the reference level of a biomarker will be obtained by determining the amount of said biomarker in a group of healthy subjects, and calculating the reference level by appropriate statistic measures including median, average, quantiles, PLS-DA, logistic regression methods, random forest classification or others that give a threshold value. The threshold value should take the desired clinical settings of sensitivity and specificity of the test into consideration.

The present invention is based on the finding that circulating sPDGFRβ levels are elevated in patients with fibrosis, in particular in patients with liver fibrosis and cirrhosis due to various causes of liver disease (alcoholic, viral, metabolic). More in particular, the inventors found that circulating sPDGFRβ levels are correlated to the stage of liver fibrosis, ranging from no or minimal fibrosis to advanced fibrosis or cirrhosis. The invention is therefore directed to the use of sPDGFRβ as a biomarker for the diagnosis or prognosis of fibrosis or for assessing the therapeutic efficacy in patients with fibrosis.

In a further aspect, the inventors found that integration of circulating sPDGFRβ levels into a novel diagnostic algorithm even improved the diagnostic accuracy of sPDGFRβ. In particular,

the PRTA score was developed combining three different factors, namely the circulating sPDGFRβ level, the albumin level and the amount of thrombocytes. Combining these three factors results into the PRTA score, using the following ratios:

PRTA score = [sPDGFRβ (pg/mL) *100]/ [albumin (g/L) * (thrombocytes (/mm^3)/100)].

The inventors here show that said PRTA score has a predictive character for significant and advanced fibrosis. Therefore, in a further embodiment, the invention is directed to the use of said PRTA score as a biomarker for the diagnosis or prognosis of fibrosis or for assessing the therapeutic efficacy in patients with fibrosis.

As said, in a first aspect of the invention, an *in vitro* method of diagnosing fibrosis in a subject is disclosed, said method comprising: a) determining the level of soluble PDGFRβ (sPDGFRβ) or calculating the PRTA score in a biological fluid test sample obtained from said subject; and b) comparing said level of sPDGFRβ or PRTA score to a reference level of sPDGFRβ or reference PRTA score that is characteristic of a healthy subject without fibrosis in order to diagnose whether the subject has fibrosis, wherein an increase in sPDGFRβ or PRTA score in the test sample compared to the reference level is indicative for fibrosis. In a further embodiment, said *in vitro* method is for diagnosing fibrosis selected from liver fibrosis, kidney fibrosis or lung fibrosis; preferably liver fibrosis.

Fibrosis refers to any of a variety of biological phenomena that are characteristic of a fibrotic cell. The phenomena can vary with the type of fibrosis, but the fibrosis phenotype is generally identified by abnormalities in scar tissue formation. For example, the chronic presence of liver-injury causing agents, including alcohol, hepatitis B or C virus (HBV/HCV) infection, and non-alcoholic steatohepatitis / fatty liver disease (NASH/NAFLD), leads to the activation of hepatic stellate cells (HSCs) toward a myofibroblastic phenotype. This activation process is characterized by an excessive deposition of extracellular matrix, scar tissue formation, and an enhanced responsiveness of the HSCs towards various stimulating factors secreted by their microenvironment, resulting in liver fibrosis. Also in said embodiment, the reference level of sPDGFRβ that is characteristic of a healthy subject without fibrosis is obtained by determining the amount of sPDGFRβ in a group of healthy subjects, preferably a group of healthy age- and sex-matched subjects.

Another aspect of the invention relates to an *in vitro* method of diagnosing the severity of fibrosis in a subject, said method comprising a) determining the level of sPDGFRβ or calculating the PRTA score in a biological fluid test sample obtained from said subject, and b) comparing said level of sPDGFRβ or PRTA score to a predetermined level of said sPDGFRβ or PRTA score in a population of subjects ranging from no fibrosis to severe fibrosis. In a further embodiment, said population of subjects ranges from no or minimal liver fibrosis (stage F0 or F1) to severe liver fibrosis or liver cirrhosis (stages F2-4). The different stages of liver fibrosis can be categorized

as follows: no liver fibrosis (F0), mild live fibrosis (F1), significant liver fibrosis (F2), advanced liver fibrosis (F3) and liver cirrhosis (F4).

In a further aspect of the invention, the levels of sPDGFRβ or the PRTA score can be used to determine the prognosis of fibrosis in a subject. To this end, the level of sPDGFRβ or the PRTA score in a biological fluid test sample obtained from said subject will be compared to a reference level of sPDGFRβ or PRTA score wherein said reference level is characteristic of a healthy subject.

In still another embodiment, an in vitro method of assessing the efficacy of a therapeutic agent against fibrosis in a subject is provided, based on the determining the level of sPDGFRβ or calculating the PRTA score at a time point before the start of treatment with a therapeutic agent against fibrosis; and at one or more time points after the start of the treatment with said agent. In said method, a decrease in the level of sPDGFRβ or in the PRTA score will be indicative for a decrease in disease progression in the subject; whereas an increase in the level of sPDGFRβ or in the PRTA score will be indicative for an increase in disease progression in the subject. The therapeutic agent against fibrosis can be any agent that is known in the field to treat the different types of fibrosis. For example, the therapeutic agent can be selected from the group comprising interferon alfa-2b, PEG-interferon alfa-2b, PEG-interferon alfa-2a, lamivudine (Epivir), adefovir (Hepsera), telbivudine (Tyzeka), entecavir (Baraclude), ribavirin, boceprivir (Victrelis), telaprevir (Incivek), simeprevir (Olysio), sofosbuvir (Sovaldi), ledispasvir/sofobuvir (Daklinza), dasbuvir, CB1 antagonist (e.g. rimonabant), 5HT-2B receptor antagonist, angiotensin-converting enzyme (ACE) inhibitor, angiotensin II type 1 (AT1) receptor blocker endothelin (ET-1) receptor antagonist, adiponectin, ghrelin, PDGF receptor antagonist, imatinib, nilotinib, tissue inhibitors of metalloproteinases (TIMPs), sulfasalazine, gliotoxin, nonsteroidal anti-inflammatory drugs (NSAIDs), and any combination thereof.

In yet another embodiment, the present invention discloses *in vitro* methods of diagnosing fibrosis, of determining the prognosis of fibrosis, or of assessing the efficacy of a therapeutic agent based on the levels of sPDGFRβ supplemented with the analysis of one or more additional biomarkers for fibrosis. In said context, the level(s) of one or more additional biomarkers are compared to the reference levels of said one or more additional biomarkers that are characteristic of a healthy subject without fibrosis in order to diagnose the presence or severity of fibrosis, or in order to determine the prognosis of fibrosis in said subject. Said one or more additional biomarkers can be any known or unknown biomarkers for fibrosis. More in particular, said biomarkers can be selected from the group comprising aspartate transaminase (AST), alanine transaminase (ALT), alkaline phosphatase, bilirubin, albumin, gamma-glutamyl transferase, creatinine, alpha-fetoprotein, the thrombocyte level, or circulating miRNAs; in

particular albumin and thrombocyte level. In another embodiment, the present invention discloses *in vitro* methods of diagnosing fibrosis, of determining the prognosis of fibrosis, or of assessing the efficacy of a therapeutic agent based on the levels of sPDGFRβ supplemented with the analysis of circulating miRNAs; preferably with the analysis of at least one circulating miRNA, even more preferably with the analysis of at least five circulating miRNAs. In still a further aspect, said circulating miRNAs are selected from miRNA-451a, miRNA-142-5p, Let-7f-5p, miRNA-378-3p, miRNA-122-5p, and miRNA-29a-3p; even more preferably selected from miRNA-451a, miRNA-142-5p, Let-7f-5p, miRNA-122-5p and miRNA-29a-3p.

In another aspect, the present application provides an in vitro method of diagnosing the presence and/or severity of fibrosis, preferably liver fibrosis, in a subject, wherein said method comprises calculating the miRFIB score, wherein the miRFIB score is calculated using the following formula: miRFIB score = 4.3799 + (0.70824 x Let-7f-5p (dCT)) – (0.090912 x miRNA-122-5-p (dCT)) – (0.26149 x miRNA-142-5p (dCT)) – (0.53602 x miRNA-29a-3p (dCT)) – (0.041140 x miRNA-451a (dCT)), wherein dCT represents the delta CT value of each specific miRNA determined using real-time PCR, and wherein said miRFIB score is compared ot the miRFIB score of a healthy subject without fibrosis.

In still a further aspect, the present invention provides an *in vitro* method of diagnosing the presence and/or severity of fibrosis; preferably liver fibrosis, in a subject, said method comprising calculating the miRFIB^{p} score and comparing the miRFIB^{p} score of said subject to the miRFIB^{p} score of a healthy subject without fibrosis, wherein the miRFIB^{p} score is calculated using the formula: miRFIB^{p}-score = (0.97229 x miRFIBscore) + (0.00021150 x PDGFRβ (pg/ml)) - 1.8678, wherein the PRTA score and the miRFIB score are calculated as disclosed herein above, and wherein the levels of sPDGFRβ and circulating miRNAs are determined in a biological fluid test sample obtained from the subject.

The level of sPDGFRβ and said biomarkers can be determined using any known technology suitable for determining the level of biomarkers in a biological fluid test sample. In a particular embodiment, the level of sPDGFRβ and/ or said biomarkers are determined using immuno-based technologies, such as enzyme-linked immunosorbent assay (ELISA), immune-chromatography, Luminex assays, CyTOF, or immunofluorescence assays.

In the context of this invention, the thrombocyte level indicates the number of thrombocyte present in the fluid sample. In a particular embodiment, the levels of the thrombocytes are determined using state-of-the-art counting technologies; in particular using an automatic microscopy-based counting technology or automated blood cell analyser.

In the different aspects of the invention, the levels of level of sPDGFRβ and/or the one or more additional biomarkers are determined in a biological fluid test sample obtained from a subject;

preferably a human subject. The term biological fluid sample includes blood, blood serum, blood plasma, saliva, urine, bone marrow fluid, cerebrospinal fluid, synovial fluid, lymphatic fluid, amniotic fluid, nipple aspiration fluid and the like. Preferred biological fluid samples for analysis are those that are conveniently obtained from patients, particularly preferred biological fluid samples are blood, blood plasma, serum or urine. Although the present invention can be carried out without pre-treatment of the sample prior to determining the level of sPDGFRβ or the one or more additional biomarkers, in a particular embodiment samples for analysis may require specific processing steps before the analysis. The precise method of sample processing employed may vary in accordance with several factors attributable to the choice of sample fluid.

EXAMPLES

EXAMPLE 1

Materials and methods

Patient population. Patients were recruited from the Department of Gastroenterology of the University Hospital of Brussels (UZ Brussel), Belgium. The study protocol was approved by the local ethical committee of the UZ Brussel and Vrije Universiteit Brussel (reference number 2015/297; B.U.N. 143201525482) and was in accordance with the Declaration of Helsinki. Patients with alcoholic, metabolic, and viral liver disease were recruited. A healthy population that had no evidence of liver disease was recruited as control group. All participants signed an informed consent prior to inclusion to the study. Diagnosis of liver fibrosis and cirrhosis was based on physical examination and elastographic techniques. Patients which presented a viral or alcoholic etiology of liver disease underwent transient elastography (FibroScan, Echosens France). Patients with at least 10 valid liver stiffness measurements with a success rate of at least 60% were included in the final analysis. Cut-off values used to discriminate fibrotic stages equal or more than F2, F3 or F4, were respectively 7.2kPa, 9.5kPa and 12.5kPa, conform to published data (Friedrich-Rust et al., 2008). Due to limited diagnostic accuracy of FibroScan in patients with excessive subcutaneous adipose tissue (Foucher et al., 2006; Sandrin et al., 2003), acoustic radiation force impulse (ARFI) was applied to determine the stage of liver fibrosis in those patients with metabolic liver disease. Cut-off values of 1,25m/s, 1,54 m/s and 1,84m/s were used to identify a fibrotic progression equal to, or more than F2, F3, and F4 respectively. Further validation of the suggested fibrosis scoring was obtained by physical examination, hematological analysis, and diagnostic algorithms such as Fib-4, APRI, and AST/ALT ratio. Fib-4 and APRI were calculated using following formulae:

FIB 4 = age × AST [IU/L]/(platelet count [10^9/L] × (ALT [IU/L])$^{1/2}$)

APRI = (AST[IU/L]/ULN)/platelet count[10^9/L]

Human liver tissue was obtained from surgical procedures carried out at the Department of Thoracic and Transplantation Surgery and Surgical Oncology of the University Hospital of Brussels (UZ Brussel), Belgium. Ethical approval was obtained from the local ethical committee

of the UZ Brussel (Reference number 2015/278; B.U.N. 143201525406) and was in accordance with the Declaration of Helsinki. All participants signed an informed consent prior to inclusion to the study.

Blood collection. Blood samples were collected by venipuncture into evacuated EDTA-KE S-Monovette tubes (Sarstedt AG & Co, Nümbrecht, Germany) prior to elastographic measurements. Blood specimens were subjected to hematological and biochemical analyses. Plasma was created within maximum 2h after collection, using a two-step centrifugation protocol consisting of 1500g for 10 min (4°C) and 2000g for 3 min (4°C). Plasma was frozen at -80°C until use.

Animal studies. The use and care of animals was reviewed and approved by the Ethical Committee of Animal Experimentation of the Vrije Universiteit Brussel (VUB, Belgium) in project 16-212-2, and was carried out in accordance to European Guidelines for the Care and Use of Laboratory Animals. Mice were housed in a controlled environment with free access to chow and water. Quiescent hepatic stellate cells were isolated from male Balb/c mice (Charles River Laboratories, L'Arbresle, France) (25-30 weeks old) as described earlier (Dekervel et al., 2017). Briefly, murine livers were perfused with enzymatic solutions, followed by low-speed centrifugation steps to remove hepatocytes. Hepatic stellate cells were purified from the non-parenchymal fraction based on their buoyancy, using an 8% Nycodenz solution. Isolated HSCs were cultured on regular tissue culture dishes (Greiner Bio-One, Vilvoorde, Belgium), in Dulbecco's modified Eagle's medium (Lonza, Verviers, Belgium) supplemented with 10% exosome-depleted fetal bovine serum (System Biosciences, Mountain View, USA), 2Mm L-glutamine (Ultraglutamine 1®) (Lonza), 100U/ml penicillin and 100µg/ml streptomycin (Pen-Strep®) (Lonza), inducing an *in vitro* myofibroblastic transdifferentiation.

The different liver cell populations were isolated based on cell-type specific protein expression, as described earlier (Stradiot et al., 2017). Briefly, murine livers were perfused with enzymatic solutions, followed by low-speed centrifugation steps to separate the non-parenchymal fraction from the hepatocyte population. The non-parenchymal fraction (NPF) was incubated with anti-F4/80-APC (MF8021, Thermo Scientific, USA) and anti-CD32-PE (ab30357, Abcam, UK). NPF was then analyzed with FACS (FACS Aria II, Becton-Dickinson, Belgium) and used to isolate liver sinusoidal endothelial cells (LSEC, CD32+F4/80-UV-), Kupffer cells (CD32-F4/80+UV-) and HSCs (CD32-F4/80-UV+).

For *in vivo* induction of liver fibrosis, 10-week old mice received 8 intraperitoneal injections of 15µl carbon tetrachloride (CCl_4) diluted in 85µl mineral oil (Sigma-Aldrich, St. Louis, MO, USA) per 30g bodyweight over a period of 4 weeks. Mice were sacrificed 24h after the last injection. `

Human Hepatic Stellate Cells. Primary human HSCs were purchased from ScienCell (San Diego, USA), and used before passage 8 was reached. The LX-2 cell line, an immortalized human HSC line, was kindly provided by Dr. Scott L. Friedman (Mount Sinai School of Medicine, New York, USA). Human HSCs were cultured in Dulbecco's modified Eagle's medium (Lonza) supplemented with 10% exosome-depleted fetal bovine serum (System Biosciences), 2Mm L-

glutamine (Ultraglutamine 1®) (Lonza), 100U/ml penicillin and 100µg/ml streptomycin (Pen-Strep®) (Lonza),

Cell-derived extracellular vesicle (EV) isolation. Conditioned media was collected from cultured mouse HSCs after 2 days or 10 days of culture (new medium was added every 2 days) and cleared from cellular debris by centrifugation at 300g for 5 min (4°C) and 2500g for 20 min (4°C). Large vesicle-like contaminants were depleted by centrifugation at 10.000g for 30 min. The supernatant was further centrifuged at 100.000g for 2 hours (4°C) to pellet EVs, which were then washed once by resuspension in phosphate-buffered saline (PBS) followed by a final ultracentrifugation step at 100.000g for 2 hours (4°C). The final EV pellet was resuspended in a small volume of PBS and characterized by use of the ZetaView® PMX110 (Particle Metrix, Meerbusch, Germany) which is equipped with nanoparticle tracking analysis (NTA) software, for particle size, zeta-potential, and concentration. The instrument was calibrated using 100nm sized polystyrene particles and handled following manufacturer's protocol. NTA measurements were executed at 11 different positions at a constant temperature of 23°C.

Immunohistochemistry. Following fixation in 4% formalin, and embedding in paraffin, liver tissues were sliced in 4µm sections. For immunohistochemical analysis, sections were deparaffinized and rehydrated through sequential washes of graded ethanol and water. Citrate buffer (pH 6,0) was used for antigen retrieval. Endogenous peroxidase was blocked by use of a 0,3% H_2O_2/methanol solution for 20 min. After permeabilization by use of 0,05% PBS-Tween, sections were blocked using 2% BSA-PBS Blocking solution. Sections were incubated overnight with following primary antibodies diluted in 1% BSA-PBS: Rabbit anti-αSMA (1:600, Ab32575 Abcam) and rabbit anti-PDGFRβ (1:100, Ab32570, Abcam). Detection was performed using anti-rabbit HRP-labelled secondary antibody (Dako, Agilent Technologies, Belgium) and DAB substrate. Sections were counterstained with Harris hematoxylin modified solution (Sigma-Aldrich, Belgium) and mounted in DPX-mounting medium.

Immunofluorescence. 4µm tissue sections were deparaffinized and rehydrated through sequential washes of graded ethanol and water. Citrate buffer (pH 6,0) was used for antigen retrieval. After permeabilization by use of 0,05% PBS-Tween, sections were blocked using 2% BSA-PBS Blocking solution. The tissue sections were incubated overnight at 4°C with rabbit anti-PDGFRβ (1:100, Ab32570, Abcam) primary antibody. Tissue sections were washed with 0,05% PBS-Tween, and simultaneously incubated with a goat anti-rabbit Alexa Fluor 488 secondary antibody (1:200, A11006, ThermoFisher) and Cy3-coupled mouse anti-αSMA primary antibody (1:100, C6198, Sigma-Aldrich) for one hour and a half. The tissue sections were finalized using DAPI-containing mountant (ProLong Gold Antifade mountant, ThermoFisher).

Sirius Red/Fast green staining. To assess collagen deposition, the paraffin-embedded liver sections were deparaffinized and rehydrated, followed by staining using Direct Red80/Fast Green FCF ((365548/F-7258, Sigma-Aldrich) in a picric acid solution for 45 min at RT and protected against light. The sections were then washed, dehydrated, and mounted with DPX

mounting medium.

Image acquisition. Whole slide images were taken using an Aperio CS2 image capture device (Leica, Diegem, Belgium). Staining were quantified using the Orbit Image Analysis software (Actelion Pharmaceuticals Ltd, Allschwil, Switzerland) (Seger et al., 2018), a free open source software which uses machine learning to identify and quantify stained tissue classes.

Immunoblotting. Extracellular vesicles, cells, and tissues were dissolved in RIPA lysis buffer (50mM Tris-HCl pH 7,4; 1% NP-40; 0,5% Na-deoxycholate; 0,1% SDS; 150mM NaCl; 2mM EDTA; 50mM NaF) supplemented with cOmplete protease-inhibitors (Roche Diagnostics, Mannheim, Germany) and PhosSTOP phosphatase-inhibitors (Roche Diagnostics). Lysates were sonicated, and protein concentrations were quantified using the Micro BCA™ Protein assay kit (Thermo Fisher Scientific) according to manufacturer's instructions. Equal amounts of proteins were subjected to SDS-PAGE and then transferred to 0.45µm PVDF membranes. Membranes were blocked with 5% fat-free milk at room temperature for 1 hour and incubated overnight at 4°C with primary antibodies including PDGFRβ (1:1000, Abcam, Cambridge, UK), αSMA (1:1000, Sigma-Aldrich, St-Louis, MO, USA), GAPDH (1:1000, Abcam), Calreticulin (1:1000, Cell Signaling Technology, Danvers, MA, USA), and HSP70 (1:200, Santa Cruz Biotechnology, Dallas, Texas, USA). Membranes were incubated with horseradish peroxidase conjugated secondary antibody (1/20000, Dako, Glostrup, Denmark) for 1 hour at room temperature. Proteins were visualized with an ECL chemiluminescence detection system (Pierce Chemical Co.). Positive immunoreactive bands were quantified by densitometrical analysis using FIJI software (Schindelin et al., 2012) and normalized to GAPDH.

Enzyme-linked immunosorbent assays (ELISA). Human soluble PDGFRβ was measured with a commercially available ELISA kit (ThermoFisher scientific), according to manufacturer's instructions. All plasma samples were diluted 1/10 with diluent provided by the manufacturer. Absorbance values were obtained with an iMark™ microplate absorbance reader (Bio-rad).

Statistical analysis. Data was analyzed using GraphPad Prism 6 (GraphPad, Palo Alto, USA) statistical software. Quantitative variables are expressed as means ± standard deviation (SD). Statistical analyses were performed using the Student's t-test, Mann-Whitney test, and Kruskal-Wallis test with Dunn's post hoc test, as appropriate. Categorical variables were analyzed using the Chi-square test. To determine the diagnostic accuracy and performance, receiver operating characteristic (ROC) curves were constructed, and the area under the curve (AUC) was calculated. In order to identify ideal cut-off values, the Youden's index was calculated (Youden, 1950), and the sensitivity and specificity were computed. Correlation studies were executed using the Spearman's correlation test. Differences of obtained results were considered significant at $p<0.05$.

Results

Human and murine aHSC-derived EVs are positive for PDGFRβ

We previously reported on the enhanced expression of PDGFRβ on extracellular vesicles (EVs)

extracted from the plasma of chronic Hepatitis B or C virus (HBV/HCV)-infected patients with early (F ≤ 2) liver fibrosis (Dekervel et al., 2017). This lead us to speculate that these circulating EVs could represent the presence of activated HSCs in the injured liver. To investigate this hypothesis, we first verified the HSC-derived origin of these PDGFRβ-positive EVs. Vesicles extracted by ultracentrifugation from the culture medium of primary mouse- and human HSCs (Thery, Amigorena, Raposo, & Clayton, 2006) show an average size of 130nm **(Figure 1A)**, which corresponds to the characteristic size of small vesicles (Raposo & Stoorvogel, 2013). Protein analysis further characterized these EVs through their positivity for the EV-marker Heat Shock Protein 70 (HSP70) and absence of the cellular marker calreticulin **(Figure 1B and C),** indicative of pure EVs. Comparison of EVs extracted from media collected from activated primary mouse HSC cultures (culture day 8-10) to more quiescent HSC cultures (day 0-2), shows an enrichment in PDGFRβ **(Figure 1B)**. In line, a strong PDGFRβ-positivity can be seen in EVs derived from activated primary human HSCs **(Figure 1C)**, but is is lacking on LX2s and their EVs **(Figure 1C)**.

PDGFRβ is up-regulated in the murine CCl_4-injury model

We next analyzed the expression of PDGFRβ in a well-established murine model of liver fibrosis, being repeated injections of carbon tetrachloride (CCl_4), in which chronic necro-inflammatory damage leads to a significant activation of HSCs (Starkel & Leclercq, 2011). Protein analysis of the livers of 4-week CCl_4-treated mice shows a significant up-regulation of PDGFRβ, both by western blot **(Figure 2A)** and on staining **(Figure 2B)**, as compared to their healthy controls. RNA expression analysis shows a dominant expression of PDGFRβ in HSCs when compared to the non-parenchymal fraction (NPF), and to other freshly isolated individual liver cell types being the hepatocytes, liver sinusoidal endothelial cells, and Kupffer cells **(Figure 2C)**. This HSC-association is further illustrated by the correlation and overlap (Spearman's correlation coefficient (r) = 0.7838) in expression of PDGFRβ and alpha smooth muscle actin (αSMA), a marker specific for activated HSCs in CCl_4-treated mice (not shown).

Human fibrotic/cirrhotic liver tissue shows elevated PDGFRβ expression

Picrosirius stainings were performed to verify the excessive collagen deposition, and thus the fibrotic/cirrhotic character of liver tissue obtained from cirrhotic HCC patients **(Figure 3)**. Collagen deposition was absent or limited in healthy liver tissue obtained from patients undergoing resection of colorectal metastases. Together with the significant deposition of collagens in the fibrotic/cirrhotic tissue, a significant higher expression of PDGFRβ can be seen **(Figure 3)**, confirming published data (Cao et al., 2010; Pinzani et al., 1996), and our observations made in the mouse model.

Study population

Due to the some drawbacks of vesicle research (Lambrecht, Verhulst, Mannaerts, Reynaert, & van Grunsven, 2018), the clinical setting is currently not ready to use EVs, nor their protein content, as biomarkers for the diagnosis of disease onset or its progression. We therefore

investigated the possibility to use total circulating PDGFRβ content as biomarker for liver fibrosis progression. For this reason, the plasma PDGFRβ-content of a cohort of 148 patients and 14 healthy volunteers was analyzed. Patients with various etiologies of liver disease were included, being chronic alcohol abuse (n = 35), chronic HBV/HCV infection (n = 46), and metabolic disease (NASH/NAFLD; n = 67) **(Table 1A)**. All cohorts did not significantly differ in terms of age and sex. As expected, a significant higher Body Mass Index (BMI) value is observed in patients with metabolic liver disease.

Patients with alcoholic or viral liver disease underwent transient elastography (Fibroscan) to diagnose the stage of fibrosis/cirrhosis. Patients with metabolic liver disease all suffered from Diabetes Mellitus 2, and where referred to the Hepatology department of the UZ Brussels due to the presence of deviant values of liver-related biochemical parameters. The presence and stage of liver fibrosis/cirrhosis in this cohort was identified by the ARFI. In the total patient cohort, stage of liver fibrosis was distributed as follows: F0-1, n = 51 (34,46%); F2, n = 29 (19,59%); F3, n = 28 (18,92%); and F4, n = 40 (27,03%). Various fibrosis scoring algorithms, including the aspartate aminotransferase/alanine aminotransferase (*AST/ALT*) *ratio*, AST to platelet ratio index (APRI), and Fibrosis-4 (Fib-4) index, were calculated to further validate the early or late disease-character of all included patients **(Table 1B)**.

sPDGFRβ predicts the presence of significant (F ≥ 2) fibrosis

ELISA-mediated analysis of soluble PDGFRβ (sPDGFRβ) levels in our total patient cohort, identified an overall increase of sPDGFRβ according to the stage of liver fibrosis **(Figure 4A)**. Creating various sub-populations based on staging of fibrosis identified a significant discriminative value of sPDGFRβ levels to distinguish patients with significant fibrosis (F ≥ 2) from those with no or minimal fibrosis (F0-1); (median [25^{th}; 75^{th} percentile]) 9317 [6625;12333] pg/mL vs 5581 [3838;10069] pg/mL, respectively, $p < 0,0001$. Use of sPDGFRβ to predict the presence of significant fibrosis (F ≥ 2) was assessed by construction of AUROC, and generated an AUC of 0,7303 (95% CI: 0,6395-0,8211) **(Table 2)**, which is considerably higher than the AUCs obtained from clinical scores such as Fib-4, APRI and AST/ALT, respectively 0,6635 (95% CI: 0,5690-0,7581), 0,6309 (95% CI: 0,5331-0,7286), and 0,5976 (95% CI: 0,4952-0,7001) **(Table 2)**. When the cut-off for parting of the patient population is taken at advanced fibrosis (F ≥ 3) or cirrhosis (F4), significant differences with lower fibrosis stages can still be seen, respectively $p = 0,0079$ and $p = 0,0273$ **(Figure 4A)**. However, the predictive character of sPDGFRβ strongly decreases (F ≥ 3: 0,6446 (95% CI: 0,5565-0,7327); F = 4: 0,6409 (95% CI: 0,5457-0,7360)) **(Table 2)** and is lower than the calculated established clinical scores **(Table 2)**.

Predictive function of sPDGFRβ is independent of disease etiology

Division of the patient cohort based on disease etiology identified the strongest discriminative function of sPDGFRβ for significant liver fibrosis (F ≥ 2) in patients with alcoholic liver disease; 0,8634 (95% CI: 0,6836-1,043) **(Table 4)**. The predictive function in patients with viral or metabolic liver disease are respectively 0,7253 (95% CI: 0,5732-0,8774) and 0,6406 (95% CI:

0,4825-0,7986). The predictive function of sPDGFRβ for significant liver fibrosis (F ≥ 2) is higher for all three disease etiologies, separately, than the predictive accuracy of Fib-4, APRI or AST/ALT **(Table 5)**, indicating the etiology-independence of the results obtained from analysis of the total population. Additionally, we did not find any association between sPDGFRβ levels and clinical features such as sex (p = 0,2863), age (r = 0,1578; p = 0,0562), and BMI (r = 0,1132; p = 0,1863).

Correlation of sPDGFRβ with metabolic and biochemical parameters

Only a few parameters had significant correlation to sPDGFRβ **(Figure 4B)**, being ALT (r = 0,1724; p = 0,0440), alkaline phosphatase (r = 0,1969; p = 0,0226), total bilirubin (r = 0,2990; p = 0,0005), and albumin (r = -0,1820; p = 0,0414). Their low correlation coefficient, and the fact that only limited number of parameters correlate with sPDGFRβ is explained by the hepatocyte-nature of most tested metabolic and biochemical parameters. This further underlines the HSC-origin of sPDGFRβ and its progressive increasing character in liver fibrosis.

Integration of sPDGFRβ into a novel diagnostic algorithm: the PRTA-score

To improve the diagnostic accuracy of sPDGFRβ, we generated an algorithm containing three factors that are all correlated with fibrosis progression **(Figure 4C)**: sPDGFRβ (r = 0,3406; p < 0,0001), albumin (r = -0,2541; p = 0,00391); and thrombocyte levels (r = -0,3343; p < 0,0001). When sPDGFRβ is combined with each individual factor, an increase in AUC can be seen for the prediction of significant fibrosis (sPDGFRβ/albumin: 0,7431; sPDGFRβ/thrombocytes: 0,7672), advanced fibrosis (sPDGFRβ/albumin: 0,6702; sPDGFRβ/thrombocytes: 0,7360), and cirrhosis (sPDGFRβ/albumin: 0,6938; sPDGFRβ/thrombocytes: 0,7701) **(Table 3)**. We combined these three factors into the PRTA-score, using the following ratios:

PRTA-score =(sPDGFRβ[pg/mL] *100)/(albumin[g/L] *(thrombocytes[/mm^3] /100))

The PRTA-score has a predictive character for significant fibrosis (0,7849 (95% CI: 0,6995-0,8702) and advanced fibrosis (0,7470 (95% CI 0,6586-0,8355), higher **(Table 3)** than those provided by Fib-4, APRI, and AST/ALT **(Table 2)**. However, the predictive function for cirrhosis (0,7995 (95% CI: 0,7122-0,8868) remains lower that the AUC obtained by using the Fib-4 score: 0,8344 (95% CI: 0,7623-0,9605).

The PRTA-score is independent of sex and BMI

The PRTA-score is independent of sex, as no significant differences (p = 0,9185) are observed between male (9,293[5,538;15,50]) and female (9,110[7,280;11,84]) patients. Additionally, no correlation has been found between BMI of the patients and outcome of the PRTA-Score (r = 0,1064; p = 0,2558).

The PRTA-score is highly predictive for significant fibrosis

We next compared the diagnostic accuracy of sPDGFRβ alone, with the PRTA-score, and with the most important, and most used, clinical score: Fib-4 scoring **(Figure 5)**. The prediction of significant fibrosis increased from 0,7303 (95% CI: 0,6395-0,8211) using sPDGFRβ alone

(Table 2) to 0,7849 (95% CI: 0,6995-0,8702) using the PRTA-score **(Table 3)**. This AUC is significantly higher than the AUC provided by Fib-4 **(Table 2)**: 0,6635 (95% CI: 0,5690-0,7581). Additionally, for prediction of significant fibrosis, using a cut-off value of 7,804 in the PRTA-score, gave good sensitivity and specificity values, respectively 77,11% and 73,17% **(Table 3)**. When the patient population is divided based on their etiology of liver disease, a comparable significant predictive function for significant liver fibrosis is seen **(Table 6)** for viral liver disease: 0,7905 (95% CI: 0,6386-0,9423); metabolic liver disease: 0,6809 (95% CI: 0,5249-0,8369); and alcoholic liver disease 0,8641 (95% CI: 0,7301-1,025), which are all higher than the AUC values obtained by the clinical algorithms **(Table 5)**. Together this data suggests that the PRTA-score is superior to Fib-4, APRI, and AST/ALT for the diagnosis of significant liver fibrosis, independent of liver disease-etiology.

Table 1A: Patient characteristics – cohorts based on etiology of liver disease

Liver disease etiology	Alcoholic	Viral	Metabolic
Individuals, n	35	46	67
Characteristics			
Age (years): median (IQR)	60,00 (53,00-63,00)	52,50 (40,75-64,25)	55,00 (52,00-64,00)
Male, n (%)	26 (74,29%)	27 (58,69%)	42 (62,69%)
BMI (kg/m^2): median (IQR)	26,23 (23,11-30,57)	24,30 (22,36-28,12)	32,68 (28,00-35,06)
Laboratory parameters: median (IQR)			
AST (IU/L)	57,00 (28,50-88,50)	40,00 (26,50-66,00)	40,00 (24,25-54,25)
ALT (IU/L)	39,00 (26,00-60,50)	42,00 (29,50-74,00)	52,50 (37,50-76,50)
Alk Phos (IU/L)	132,0 (89,00-173,8)	70,00 (57,25-85,50)	81,00 (62,00-108,0)
GGT (IU/L)	229,0 (81,25-951,0)	47,50 (19,25-137,8)	64,00 (39,25-139,0)
Total bilirubin (mg/dL)	1,170 (0,5650-2,745)	0,6700 (0,4500-0,8800)	0,6600 (0,5700-0,9050)
Albumin (g/L)	39,00 (31,00-42,00)	43,50 (41,00-45,75)	43,00 (40,15-44,00)
Thrombocytes ($x10^3/mm^3$)	165,00 (118,25-213,75)	205,00 (156,00-256,00)	231,00 (201,00-267,00)
Creatinine (mg/dL)	0,8050 (0,6825-1,110)	0,8400 (0,7300-1,000)	0,8100 (0,700-0,9700)
Fibrosis scoring: median (IQR)			
AST/ALT ratio	1,200 (0,8931-2,226)	0,9143 (0,7905-1,167)	0,6747 (0,6137-0,8143)
APRI	0,7362 (0,4313-1,561)	0,4951 (0,3422-0,7068)	0,2985 (0,2337-0,3815)
Fib-4	2,860 (1,335-5,440)	1,900 (1,050-2,800)	1,280 (0,8600-1,700)
Fibroscan (kPa)	11,65 (6,025-51,78)	7,150 (4,600-11,78)	/
ARFI (m/s)	/	/	1,320 (1,205-1,595)

n: number; IQR: Interquartile range; BMI: Body Mass Index; AST: aspartate aminotransferase; ALT: alanine aminotransferase; Alk Phos: Alkaline phosphatase; GGT: gamma-glutamyl transferase; Fib-4: Fibrosis-4; AST/ALT-ratio: aspartate aminotransferase/alanine aminotransferase ratio; APRI: AST to platelet ratio index; ARFI: acoustic radiation force impulse

Table 1B: Patient characteristics – cohorts based on elastography-determined F-stage

	F0-F1	F2	F3	F4
Individuals, n	51	29	28	40
Characteristics				
Age (years): median (IQR)	52,00 (46,00-61,00)	57,00 (51,00-65,50)	55,00 (51,25-61,00)	60,00 (54,00-65,75)
Male, n (%)	28 (54,90%)	13 (44,82%)	22 (78,57%)	32 (80,00%)
BMI (kg/m^2): median (IQR)	26,86 (23,51-32,33)	32,12 (28,41-35,05)	28,04 (25,02-34,89)	26,89 (23,69-31,59)
Laboratory parameters: median (IQR)				
AST (IU/L)	39,00 (24,00-51,00)	35,00 (23,50-35,00)	41,50 (28,25-62,00)	58,00 (39,75-92,50)
ALT (IU/L)	43,00 (32,00-65,00)	45,00 (31,50-69,50)	52,50 (33,00-77,00)	47,50 (30,75-47,50)
Alk Phos (IU/L)	70,50 (56,50-90,50)	91,00 (70,50-109,0)	74,00 (65,00-86,00)	134,0 (89,00-182,5)
GGT (IU/L)	62,00 (29,50-140,5)	64,00 (35,50-116,0)	53,00 (43,00-133,0)	189,0 (106,3-593,0)
Total bilirubin (mg/dL)	0,6100 (0,5400-0,7650)	0,5500 (0,3900-0,8350)	0,6950 (0,6400-1,113)	1,060 (0,7175-2,818)
Albumin (g/L)	43,00 (41,00-45,00)	42,50 (40,00-44,75)	42,00 (38,50-45,50)	40,00 (32,00-43,75)
Thrombocytes ($x10^3/mm^3$)	232,0 (179,0-273,5)	226,5 (181,8-263,5)	227,0 (158,3-269,0)	167,5 (84,50-218,5)
Creatinine (mg/dL)	0,7700 (0,6550-0,9975)	0,8750 (0,6975-1,010)	0,8250 (0,7800-0,9600)	0,8400 (0,7000-1,100)
Fibrosis scoring: median (IQR)				
AST/ALT ratio	0,7797 (0,6250-1,019)	0,8125 (0,7021-0,9615)	0,7619 (0,250-1,031)	1,200 (0,8105)
APRI	0,3453 (0,2406-0,4567)	0,3817 (0,2434-0,5138)	0,3467 (0,2490-0,5338)	0,9809 (0,4085-1,685)
Fib-4	1,225 (0,9317-1,806)	1,425 (0,7900-2,215)	1,460 (0,8922-2,710)	2,920 (1,770-6,020)
Fibroscan (kPa)	5,000 (4,000-5,750)	8,150 (7,650-8,7000)	11,00 (9,675-11,78)	30,30 (16,80-65,30)
ARFI (m/s)	1,150 (1,115-1,180)	1,285 (1,260-1,510)	1,615 (1,573-1,798)	1,950 (1,870-2,043)

n: number; IQR: Interquartile range; BMI: Body Mass Index; AST: aspartate aminotransferase; ALT: alanine aminotransferase; Alk Phos: Alkaline phosphatase; GGT: gamma-glutamyl transferase; Fib-4: Fibrosis-4; AST/ALT-ratio: aspartate aminotransferase/alanine aminotransferase ratio; APRI: AST to platelet ratio index; ARFI: acoustic radiation force impulse

Table 2: Accuracy of sPDGFRβ and the clinical scores Fib-4, APRI, and AST/ALT-ratio for the detection of significant fibrosis (F ≥ 2), advanced fibrosis (F ≥ 3), and cirrhosis (F = 4), in the total patient cohort.

	AUC	95% CI	p-value	Optimal Cut-off	Sensitivity (%)	Specificity (%)	Youden's index
sPDGFRb							
All patients							
F ≥ 2	0,7303	0,6395 to 0,8211	< 0,0001	6003	82,47	62,00	0,4447
F ≥ 3	0,6446	0,5565 to 0,7327	0,002552	5861	82,35	40,51	0,2286
F = 4	0,6409	0,5457 to 0,7360	0,008703	7497	75,00	48,60	0,2360
Fib-4							
All patients							
F ≥ 2	0,6635	0,5690 to 0,7581	0,002295	1,495	65,52	68,18	0,3370
F ≥ 3	0,7123	0,6225 to 0,8022	< 0,0001	1,495	74,58	62,5	0,3708
F = 4	0,8344	0,7623 to 0,9065	< 0,0001	1,495	93,94	59,18	0,5312
APRI							
All patients							
F ≥ 2	0,6309	0,5331 to 0,7286	0,01466	0,4849	44,83	79,55	0,2438
F ≥ 3	0,6723	0,5779 to 0,7667	0,0007139	0,5718	44,07	87,5	0,3157
F = 4	0,7965	0,7028 to 0,8902	< 0,0001	0,7002	60,61	90,82	0,5143
AST/ALT ratio							
All patients							
F ≥ 2	0,5976	0,4952 to 0,7001	0,07019	1,174	28,41	90,7	0,1911
F ≥ 3	0,6423	0,5462 to 0,7383	0,005081	1,174	39,34	92,86	0,3220
F = 4	0,7486	0,6458 to 0,8515	< 0,0001	1,184	55,88	91,75	0,4763

Fib-4: Fibrosis-4; AST/ALT-ratio: aspartate aminotransferase/alanine aminotransferase ratio; APRI: AST to platelet ratio index; AUC: Area under the curve; CI: Confidence interval.

Table 3: Accuracy of sPDGFRβ, sPDGFRβ/albumin, sPDGFRβ/thrombocyte numbers, and PRTA-score for the detection of significant fibrosis (F ≥ 2), advanced fibrosis (F ≥ 3), and cirrhosis (F = 4), in the total patient cohort. (AUC: area under the curve; CI: confidence interval)

	AUC	95% CI	p-value	Optimal Cut-off	Sensitivity (%)	Specificity (%)	Youden's index
sPDGFRb							
All patients							
F ≥ 2	0,7303	0,6395 to 0,8211	< 0,0001	6003	82,47	62,00	0,4447
F ≥ 3	0,6446	0,5565 to 0,7327	0,002552	5861	82,35	40,51	0,2286
F = 4	0,6409	0,5457 to 0,7360	0,008703	7497	75,00	48,60	0,2360
sPDGFRb/albumin							
All patients							
F ≥ 2	0,7431	0,6494 to 0,8369	< 0,0001	140,0	85,88	54,76	0,4064
F ≥ 3	0,6702	0,5771 to 0,7633	0,001004	253,4	49,12	77,14	0,2626
F = 4	0,6938	0,5902 to 0,7973	0,001079	253,4	59,38	73,68	0,3306
sPDGFRb/thrombocytes							
All patients							
F ≥ 2	0,7672	0,6808 to 0,8535	< 0,0001	3,707	69,32	77,27	0,4659
F ≥ 3	0,7360	0,6487 to 0,8233	< 0,0001	4,039	75,00	70,83	0,4583
F = 4	0,7701	0,6780 to 0,8622	< 0,0001	4,589	76,47	74,49	0,5096
PRTA-score							
All patients							
F ≥ 2	0,7849	0,6995 to 0,8702	< 0,0001	7,804	77,11	73,17	0,5028
F ≥ 3	0,7470	0,6586 to 0,8355	< 0,0001	9,979	70,91	78,26	0,4917
F = 4	0,7995	0,7122 to 0,8868	< 0,0001	11,01	80,65	74,19	0,5484

Table 4: Accuracy of sPDGFRβ for the detection of significant fibrosis (F ≥ 2), advanced fibrosis (F ≥ 3), and cirrhosis (F = 4), in patient cohorts with same etiology of liver disease.

	AUC	95% CI	p-value	Optimal Cut-off	Sensitivity (%)	Specificity (%)	Youden's index
sPDGFRb							
HBV/HCV							
F ≥ 2	0,7253	0,5732 to 0,8774	0,009669	5992	73,91	72,73	0,4664
F ≥ 3	0,7429	0,5982 to 0,8876	0,005844	10951	47,37	92,31	0,3968
F = 4	0,7130	0,5284 to 0,8975	0,05030	11098	55,56	86,11	0,4167
NASH/NAFLD							
F ≥ 2	0,6406	0,4825 to 0,7986	0,07224	6249	88,89	50	0,3889
F ≥ 3	0,6015	0,4609 to 0,7421	0,1712	6321	88	32,5	0,205
F = 4	0,5918	0,4088 to 0,7748	0,3586	10116	60	65,45	0,2545
ALD							
F ≥ 2	0,8634	0,6836 to 1,043	0,002055	5520	96,3	75	0,7130
F ≥ 3	0,6612	0,4443 to 0,8782	0,1221	5520	95,65	50	0,4565
F = 4	0,6616	0,4651 to 0,8581	0,1098	5520	95,24	42,86	0,3810

AUC: Area under the curve; CI: Confidence interval; HBV: Hepatitis B virus; HCV: Hepatitis C virus; NASH: Non-alcoholic steatohepatitis; NAFLD: Non-alcoholic fatty liver disease; ALD: Alcoholic Liver disease

Table 5: Accuracy of the clinical scores Fib-4, APRI, and AST/ALT-ratio for the detection of significant fibrosis (F ≥ 2), advanced fibrosis (F ≥ 3), and cirrhosis (F = 4), in patient cohorts with same etiology of liver disease.

	AUC	95% CI	p-value	Optimal Cut-off	Sensitivity (%)	Specificity (%)	Youden's index
Fib-4							
HBV/HCV							
F ≥ 2	0,6979	0,5259 to 0,8698	0,03615	1,530	81,82	64,71	0,4653
F ≥ 3	0,7196	0,5517 to 0,8874	0,01941	1,675	83,33	61,9	0,4523
F = 4	0,7833	0,6286 to 0,9381	0,01494	1,990	87,5	66,67	0,5417
NASH/NAFLD							
F ≥ 2	0,5493	0,3939 to 0,7048	0,5430	1,355	52,5	68,42	0,2092
F ≥ 3	0,5282	0,3777 to 0,6787	0,7246	0,8450	90	28,21	0,1821
F = 4	0,6934	0,5402 to 0,8465	0,1231	1,480	83,33	64,15	0,4748
ALD							
F ≥ 2	0,8050	0,6147 to 0,9953	0,01042	2,055	76	87,5	0,635
F ≥ 3	0,8611	0,7216 to 1,001	0,0006654	2,605	76,19	91,67	0,6786
F = 4	0,8703	0,7423 to 0,9983	0,0003365	2,605	78,95	85,71	0,6466
APRI							
HBV/HCV							
F ≥ 2	0,6070	0,4248 to 0,7891	0,2573	0,4196	72,73	58,82	0,3155
F ≥ 3	0,6614	0,4863 to 0,8365	0,08577	0,4196	77,78	57,14	0,3492
F = 4	0,6774	0,4458 to 0,9090	0,1260	0,7713	50	87,1	0,3710
NASH/NAFLD							

F ≥ 2	0,6145	0,4651 to 0,7638	0,1582	0,3680	35	89,47	0,2447
F ≥ 3	0,5359	0,3839 to 0,6879	0,6539	0,3766	85	30,77	0,1577
F = 4	0,5409	0,3295 to 0,7523	0,7444	0,2967	83,33	52,83	0,3616
ALD							
F ≥ 2	0,7700	0,5637 to 0,9763	0,02334	0,5128	76	87,5	0,6350
F ≥ 3	0,8333	0,6765 to 0,9902	0,001678	0,6892	80,95	91,67	0,7262
F = 4	0,8609	0,7230 to 0,9988	0,0004748	0,6892	84,21	85,71	0,6992
AST/ALT ratio							
HBV/HCV							
F ≥ 2	0,5328	0,3457 to 0,7200	0,7238	0,8595	68,18	50	0,1818
F ≥ 3	0,5152	0,3297 to 0,7006	0,8704	1,173	33,33	86,36	0,1969
F = 4	0,5234	0,2838 to 0,7630	0,8392	1,297	37,5	90,63	0,2813
NASH/NAFLD							
F ≥ 2	0,6418	0,4709 to 0,8127	0,09399	0,6180	82,05	52,94	0,3499
F ≥ 3	0,5299	0,3774 to 0,6824	0,7097	0,6914	66,67	51,43	0,1810
F = 4	0,5896	0,3880 to 0,7911	0,3963	0,6300	88,89	40,82	0,2971
ALD							
F ≥ 2	0,8050	0,6081 to 1,002	0,01042	1,112	80	87,5	0,6750
F ≥ 3	0,8849	0,7425 to 1,027	0,0002861	1,112	90,48	83,33	0,7381
F = 4	0,8684	0,7367 to 1,000	0,0003607	1,182	84,21	78,57	0,6278

Fib-4: Fibrosis-4; AST/ALT-ratio: aspartate aminotransferase/alanine aminotransferase ratio; APRI: AST to platelet ratio index; AUC: Area under the curve; CI: Confidence interval; HBV: Hepatitis B virus; HCV: Hepatitis C virus; NASH: Non-alcoholic steatohepatitis; NAFLD: Non-alcoholic fatty liver disease. ALD: Alcoholic Liver disease

Table 6: Accuracy of sPDGFRβ-containing PRTA-score for the detection of significant fibrosis (F ≥ 2), advanced fibrosis (F ≥ 3), and cirrhosis (F = 4), in patient cohorts with same etiology of liver disease.

	AUC	95% CI	p-value	Optimal Cut-off	Sensitivity (%)	Specificity (%)	Youden's index
PRTA-score							
HBV/HCV							
F ≥ 2	0,7905	0,6386 to 0,9423	0,003340	7,748	71,43	86,67	0,5810
F ≥ 3	0,8390	0,6997 to 0,9783	0,0005253	10,43	64,71	100	0,6471
F = 4	0,8214	0,6557 to 0,9871	0,006172	10,43	75	82,14	0,5714
NASH/NAFLD							
F ≥ 2	0,6809	0,5249 to 0,8369	0,02928	7,321	79,49	55,56	0,3505
F ≥ 3	0,6136	0,4546 to 0,7725	0,1652	9,979	63,16	71,05	0,3421
F = 4	0,6667	0,4520 to 0,8813	0,1849	11,70	66,67	78,43	0,4510
ALD							
F ≥ 2	0,8641	0,7031 to 1,025	0,002501	7,738	91,3	75	0,6630
F ≥ 3	0,7675	0,5877 to 0,9474	0,01340	10,45	84,21	66,67	0,5088
F = 4	0,7983	0,6390 to 0,9576	0,004847	10,45	88,24	64,29	0,5253

AUC: Area under the curve; CI: Confidence interval; HBV: Hepatitis B virus; HCV: Hepatitis C virus; NASH: Non-alcoholic steatohepatitis; NAFLD: Non-alcoholic fatty liver disease; ALD: Alcoholic Liver disease

EXAMPLE 2

Materials and methods

Animal studies

The use and care of animals was reviewed and approved by the Ethical Committee of Animal Experimentation of the Vrije Universiteit Brussel (Brussels, Belgium) in project 16-212-2, and was carried out in concordance to European Guidelines for the Care and Use of Laboratory Animals. All mice were housed in a controlled environment with free access to water and chow. Primary HSCs were isolated from male Balb/c mice aged 25 to 30 weeks (Charles River Laboratories, L'Arbresle, France), as described earlier (Guimaraes, Empsen, Geerts, & van Grunsven, 2010; Lambrecht et al., 2017). Briefly, murine livers were digested by enzymatic solutions consisting of collagenase (Roche diagnostics, Mannheim, Germany) and pronase E (Merck, Darmstadt, Germany). The resulting cell suspension was centrifuged at low speed to remove hepatocytes. Hepatic stellate cells (HSCs) were purified from the non-parenchymal fraction based on their buoyancy, using an 8% Nycodenz (Axis-shield PoC AS, Dundee, Scotland) solution. Isolated HSCs were cultured on regular tissue culture dishes (Greiner Bio-One, Vilvoorde, Belgium), in Dulbecco's modified Eagle's medium (Lonza, Verviers, Belgium) supplemented with 10% foetal bovine serum (Lonza, Verviers, Belgium), 2 mM L-glutamine (Ultraglutamine 1®) (Lonza), 100 U/mL penicillin and 100 µg/mL streptomycin (Pen-Strep®) (Lonza), inducing *in vitro* myofibroblastic transdifferentiation. Cell purity was confirmed by the presence of lipid droplets and staining for HSC-specific markers.

For *in vivo* induction of liver fibrosis, 10-week old mice received 8 intraperitoneal injections of 15µL carbon tetrachloride (CCl_4) diluted in 85µL mineral oil (Sigma-Aldrich, St. Louis, MO, USA) per 30g bodyweight over a period of 4 weeks. Mice were sacrificed 24h after the last injection.

Patient cohort

Patients with liver fibrosis caused by chronic alcohol abuse and chronic viral hepatitis were recruited from the Department of Gastroenterology and Hepatology of the University Hospital of Brussels (UZ Brussel), Belgium. The extent of liver fibrosis in these patients was determined based on transient elastography (FibroScan®, Echosens, France). Patients with at least 10 valid stiffness measurements with a success rate of minimum 60% were included in the final analysis. Cut-off values used to discriminate fibrotic stages equal to, or more than F2, F3, and F4, were taken at 7.2 kPa, 9.5 kPa, and 12.5 kPa (Friedrich-Rust et al., 2008) respectively. Patients with liver fibrosis suffering from NAFLD were recruited from the Diabetes Centre of the University Hospital of Brussels (UZ Brussel, Brussels, Belgium) in collaboration with the Department of Gastroenterology and Hepatology (UZ Brussel, Brussels, Belgium). In these patients, the extent of fibrosis was determined by use of acoustic radiation force impulse (ARFI), using cut-off values of 1.25 m/s, 1.54 m/s, and 1.84 m/s to identify a fibrotic stage equal to, or more than F2, F3, and F4 respectively. All NAFLD-patients had Diabetes Mellitus type 2. The protocol of this study was

approved by the local ethical committee of the UZ Brussel and Vrije Universiteit Brussel (reference number 2015/297; B.U.N. 143201525482) and was in accordance with the Declaration of Helsinki. An informed consent was obtained from all participants, prior to inclusion in the study.

Blood collection

Blood samples were collected by venepuncture into evacuated EDTA-KE S-Monovette tubes (Sarstedt AG & Co, Nümbrecht, Germany) on the day of FibroScan or ARFI. All samples were subjected to haematological and biochemical analyses. Plasma was created within a maximum timespan of 2 hours after collection, using a two-step centrifugation protocol of 1500 g for 10 min (4 °C), followed by 2000 g for 3 min (4 °C). Plasma was frozen at -80 °C until further use.

Serological scoring of fibrosis

Haematological analyses and subsequent serological scoring algorithms such as our recently developed PRTA-score (Lambrecht et al., 2019) and the clinical algorithms Fib-4, APRI, and AST/ALT ratio were used to validate the elastography-based fibrosis scoring. The PRTA-score, Fib-4 and APRI were calculated using following formulae:

Fib-4 = age x AST[IU/L] / (thrombocytes[10^9/L] x (ALT[IU/L])$^{1/2}$)

APRI = (AST[IU/L] / ULN) / thrombocytes[10^9/L]

PRTA-score =(sPDGFRβ[pg/mL] *100)/(albumin[g/L] *(thrombocytes[/mm^3] /100))

Extracellular vesicle isolation and RNA extraction

Primary mouse quiescent HSCs were cultured in Dulbecco's modified Eagle's medium (Lonza, Verviers, Belgium) supplemented with 10% exosome-depleted foetal bovine serum (Lonza, Verviers, Belgium), 2 mM L-glutamine (Ultraglutamine 1®) (Lonza), 100 U/mL penicillin and 100 µg/mL streptomycin (Pen-Strep®) (Lonza). Conditioned medium was collected after 2 days or 10 days of culture. New medium was added every 2 days. Cellular debris was removed by centrifugation at 300 g for 5 min (4 °C) and 2500 g for 20 min (4 °C). Microvesicles were pelleted by centrifugation at 10,000 g for 30 min (4 °C). The supernatant was further centrifuged at 100,000 g for 2 h (4 °C) to pellet small extracellular vesicles (sEVs), which were then washed once by resuspension in PBS, followed by a final centrifugation step at 100,000 g for 2 h (4 °C). Microvesicle and sEV pellets were resuspended in a small volume of PBS. Purity of the vesicle suspensions were verified by analysis of size using the ZetaView® PMX110 (Particle Metrix, Meerbusch, Germany) and presence of specific vesicle markers using western blot, as shown previously (Lambrecht et al., 2019).

The obtained microvesicle and sEV suspensions were depleted from contaminating proteins by incubation with 0.5 mg proteinase K (ThermoFisher scientific) for 30 min at 55 °C. Total RNA

was extracted by use of the Quick RNA miniprep (Zymo Research, CA, USA). Synthetic spike-in ath-miRNA-159a, cel-miRNA-248 and osa-miRNA-414 were added to the vesicle lysates before proceeding with the manufacturer's protocol.

Nanostring miRNA analysis

The RNA samples obtained from extracellular vesicles (microvesicles and sEVs) extracted from qHSCs (day 2) and aHSC (day 10) were submitted to the BRIGHTcore facility of the Vrije Universiteit Brussel (VUB) for further processing by the NanoString nCounter system (NanoString, Washington, USA). The nCounter Mouse v1.5 miRNA panel was used, which can analyse the expression of up to 578 endogenous miRNAs. Raw counts were obtained and analysed using the nSolver software. The background threshold was determined using the geometric mean of negative control counts. For technical variations, normalization was based on the geometric mean of the spike-in ath-miRNA-159a, cel-miRNA-248 and osa-miRNA-414. Normalized counts were imported into RStudio (https://www.rstudio.com) and selected highly expressed miRNAs (sum of all counts per miRNA > 800). These miRNA expression values were scaled per miRNA and visualized using heatmap with R package "gplots".

miRNA targets were predicted using TargetScan (http://www.targetscan.org/), miRDB (http://www.mirdb.org/), starBase (http://starbase.sysu.edu.cn/), and miRTarBase (http://mirtarbase.mbc.nctu.edu.tw/). Target lists were imported into RStudio, merged together and visualized using Venn diagram with R package "gplots".

Messenger RNA and microRNA analysis

miRNAs were extracted from 500µl human- or 150µl mouse-plasma by use of the Nucleospin® miRNA Plasma kit (Macherey-Nagel, Düren, Germany) using the manufacturers protocol. Caenorhabditis elegans miRNA-39 (Cel-miRNA-39) (Qiagen, Hilden, Germany) was added into the plasma lysate before start of the extraction protocol and served as an external processing control. Total RNA from liver tissue and cultured hepatic stellate cells was extracted by respectively TRIzol reagent (ThermoFisher scientific, Waltham, USA) and ReliaPrep™ RNA Miniprep system (Promega, Madison, WI, USA), using the manufacturers protocol. Messenger RNA (mRNA) was reverse-transcribed into complementary DNA (cDNA) using a mixture of hexamer random primers, M-MLV RT Buffer, dNTP mix, M-MLV RT RNase (H-) Point mutant, and RNasin® Plus RNase Inhibitor (Promega). MicroRNA (miRNA) was reverse transcribed into cDNA using the miScript II RT kit (Qiagen, Hilden, Germany). The expression profiles of selected mRNA and miRNAs were analysed by quantitative real-time polymerase chain reaction (qPCR), using respectively GoTaq qPCR Master Mix with BRYT green (Promega) and miScript SYBR Green PCR kit (Qiagen) in the QuantStudio 3 real-time PCR system (ThermoFisher scientific). Obtained results were analysed using the QuantStudio 3 Design and Analysis Software (ThermoFisher scientific). Individual gene and miRNA expression was normalized to Gapdh, RNU6 or Cel-miRNA-39, as appropriate. Relative expression was calculated using the

comparative Ct method ($2^{-\Delta\Delta CT}$). miRNA- (Table 7) and gene- (Table 8) specific primers were produced by Integrated DNA Technologies (IDT, Leuven, Belgium).

Table 7. miRNA primers

	Accession number		Primer sequence (5′-3′)	SEQ ID NO
	Mouse	Human		
miRNA-122-5p	MIMAT0000246	MIMAT0000421	TGGAGTGTGACAATGGTGTTG	1
miRNA-29a-3p	MIMAT0000535	MIMAT0000086	TAGCACCATCTGAAATCGGTTA:	2
miRNA-202-5p	MIMAT0004546	MIMAT0002810	TTCCTATGCATATACTTCTT	3
miRNA-30b-5p	MIMAT0000130	MIMAT0000420	TGTAAACATCCTACACTCAGCT	4
miRNA-205-5p	MIMAT0000238	MIMAT0000266	TCCTTCATTCCACCGGAGTCTG	5
miRNA-451a	MIMAT0001632	MIMAT0001631	AAACCGTTACCATTACTGAGTT	6
miRNA-142-5p	MIMAT0000154	MIMAT0000433	CATAAAGTAGAAAGCACTACT	7
Let-7f-5p	MIMAT0000525	MIMAT0000067	TGAGGTAGTAGATTGTATAGTT	8
miRNA-378a-3p	MIMAT0003151	MIMAT0000732	ACTGGACTTGGAGTCAGAAGG	9
miRNA-200b-3p	MIMAT0000233	MIMAT0000318	TAATACTGCCTGGTAATGATGA	10
miRNA-377-3p	MIMAT0000741	MIMAT0000730	ATCACACAAAGGCAACTTTTGT	11
RNU6	/	/	ACGCAAATTCGTGAAGCGTT	12
Cel-miRNA-39-3	/	/	AGCTGATTTCGTCTTGGTAATA	13

Table 8. mRNA primers

	Forward primer Primer sequence (5′-3′)	SEQ ID NO	Revers primer Primer sequence (5′-3′)	SEQ ID NO
Peg10	TGCTTGCACAGAGCTACAGTC	14	AGTTTGGGATAGGGGCTGCT	15
Surf4	ATGGGACAGAACGACCTGATG	16	GGTGTCGATATAGTCACGCTG	17
Aw549877	GGCTCACATACAGCACCTTAG	18	AGTCCTCTGGAAAATCCTCATCT	19
Zfp516	ACCGGACAGGAACTCTGATTC	20	GAGGTGCTCTTAGTAGGGCTG	21
Ankrd52	CCAGGCCATCTTTAGCCGAG	22	ATGCAATGGGGTTCGCCTC	23
Atxn713	TTGTCTGGCCTGGATAACAGC	24	CCGGTGTACTTCAAAGCAGAATC	25
Ppp3r1	GAAGGAGTGTCTCAGTTCAGTG	26	ACGAAAAGCAAACCTCAACTTCT	27
Aff4	ATGAACCGTGAAGACCGGAAT	28	TGCTAGTGACTTTGTATGGCTCA	29
Dnajc27	ACGCCGAAGTGGGGAAAAG	30	GAAGAAGGGATGTCCAGCCAT	31
Ctsb	TCCTTGATCCTTCTTTCTTGCC	32	ACAGTGCCACACAGCTTCTTC	33
Clcn5	GAGGAGCCAATCCCTGGTGTA	34	TTGGTAATCTCTCGGTGCCTA	35
Cpeb3	ATCTCGCCGCTCAAAAAGC	36	GGAAAGCGTTATCCTCCATCCA	37
Gnai3	CCAGACCAACTACATTCCAACTC	38	AATTGCTGTCACTCCCTCAAAA	39
Acta2	CCAGCACCATGAAGATCAAG	40	TGGAAGGTAGACAGCGAAGC	41
Col1a1	ACCTAAGGGTACCGCTGGA	42	ACCTAAGGGTACCGCTGGA	43
Gapdh	TCGAGATCGCCACCTACAG	44	GTCTGTACAGGAATGGTGATGC	45
Lox	CTCCTGGGAGTGGCACAG	46	CTTGCTTTGTGGCCTTCAG	47

Histological evaluation

Four-micrometre paraffin-embedded liver tissue sections were cut, deparaffinized, and rehydrated before staining with Sirius Red/Fast Green or Hematoxyline/Eosin. The sections were then washed, dehydrated, and mounted with DPX mounting medium. Whole slide images were taken using the Aperio CS2 image capture device (Leica, Diegem, Belgium). Collagen staining was quantified using the Orbit Image Analysis software (Actelion Pharmaceuticals Ltd, Allschwil, Switzerland) (Seger et al., 2018).

Immunocytochemistry

After isolation of primary murine hepatic stellate cells, the cells were cultured on coverslips for 24 hours or 10 days. Cells were washed with PBS and fixed with formalin for 10 minutes. The cells were then washed three times with PBS and stored at 4°C until further use. Prior to staining, the cells were permeabilized using PBS supplemented with 0.1% Triton-X (3 x 5 minutes). Afterwards, cells were incubated for 30 minutes with 0.1% Triton-X PBS containing 2% BSA, to block non-specific binding sites. The cells were incubated overnight at 4 °C with anti-Desmin (1:200, RB-9014-P, ThermoFisher scientific), or anti-Vimentin (1:200, V5255, Sigma-Aldrich). Three wash-steps using 0.1% Triton-X PBS were applied, followed by incubation with donkey anti-rabbit Alexa Fluor 488 secondary antibody (1:200, A21206, ThermoFisher scientific), donkey anti-mouse Alexa Fluor 488 secondary antibody (1:200, A21202, ThermoFisher scientific) or Cy3-coupled mouse anti-αSMA primary antibody (1:100, C6198, Sigma-Aldrich) for one hour and a half. Coverslips were mounted with DAPI-containing mounting medium (Dako, Denmark). Images were taken using the EVOS FL fluorescence microscope (ThermoFisher).

Simultaneous isolation of different liver cell types

Liver cell populations were isolated based on the expression of cell-type specific markers, as described earlier (Stradiot et al., 2017). In summary, murine liver were digested using enzymatic solutions consisting of collagenase (Roche diagnostics, Mannheim, Germany) and pronase E (Merck, Darmstadt, Germany). The resulting cell suspension was used in low-speed centrifugation steps to separate the non-parenchymal fraction from the hepatocytes. Next, the non-parenchymal fraction (NPF) was incubated with anti-F4/80-APC (MF8021, Thermo Scientific, USA) and anti-CD32-PE (ab30357, Abcam, UK). NPF was then analysed with FACS (FACS Aria II, Becton-Dickinson, Belgium) and used to isolate liver sinusoidal endothelial cells (LSEC, CD32+F4/80-UV-), Kupffer cells (CD32-F4/80+UV-) and HSCs (CD32-F4/80-UV+).

Statistical analysis

Data was analysed using GraphPad Prism 8 (GraphPad, Palo Alto, USA). Quantitative variables are expressed as means ± standard error of the mean (SEM) or expressed as boxplots using the Tukey representation. Statistical analyses were performed using the Student's t-test, Mann-Whitney test, and One-Way ANOVA with Dunnett post hoc test, as appropriate. Categorical values were analysed using the Chi-square test. The diagnostic accuracy and performance of mentioned miRNAs and serological scores were determined using receiver operating characteristics (ROC) curves, and the area under the curve (AUC) was calculated. Sensitivity and specificity were calculated based on the highest Youden's index values (Youden, 1950). Correlation studies were executed using the Spearman's correlation test. Logistic regression analyses were performed using MedCalc version 18 (MedCalc Software, Ostend, Belgium). The sufficiency of the sample size was confirmed by MedCalc version 18 using in house preliminary results and a type I error rate (α) of 5% and a power (1-β) of 80%. Results were considered statistically significant when $p < 0.05$.

Results

Identification of candidate HSC-linked miRNAs

As hepatic stellate cell (HSC) activation is an early event of liver fibrosis initiation and progression, we hypothesized that HSC-derived circulating miRNAs could be suitable markers for early stage liver fibrosis. In order to identify candidate miRNAs, NanoString analysis was performed on extracellular vesicles (EVs), both microvesicles and small extracellular vesicles (sEV), obtained from the conditioned medium of *in vitro* activating primary murine HSCs. To this end primary mouse HSCs are plated on plastic tissue culture dishes for 10 days. Activation of cultured HSCs was verified on protein level by the up-regulation of HSC-activation markers Desmin, α-SMA, and Vimentin (data not shown), and on mRNA level by *Acta2*, *Col1a1* and *Lox* (Figure 6A). Although the obtained miRNA counts by NanoString analysis were insufficient to compare between the quiescent and activated conditions, several miRNAs were found to be highly enriched in such EVs, as compared to the average expression level of all tested miRNAs. This list of highly shed miRNAs, and thus potential fibrosis markers, was further restricted to the miRNAs that are conserved among mouse and human, to ensure translational value, ending up with a list of 9 candidate miRNAs (data not shown). Expression levels of these miRNAs were analysed in the *in vitro* activated primary mouse HSC cultures. Expression analysis of all 9 candidate miRNAs was performed by using qPCR on cell lysate of activated HSCs, as compared to freshly isolated HSCs (data not shown), and identified the significant dysregulation of 4 miRNAs: miRNA-451a, miRNA-142-5p, Let-7f-5p, and miRNA-378a-3p (Figure 6B).

Identification of Ankrd52, Clcn5 and Peg10 as potential target genes

To investigate a potential function of miRNA-451a, miRNA-142-5p, Let-7f-5p, and miRNA-378a-3p in the HSC-activation process, a bioinformatics-based target prediction was carried out, using four different predictive algorithms: TargetScan, miRDB, starBase, and miRTarBase. Of all putative targets, thirteen genes are suggested to have all four miRNAs as post-transcriptional regulators (Figure 7A). Analysis of mRNA expression in activated HSCs, compared to freshly isolated quiescent HSCs, identified 3 genes that remain stable during the activation process (Figure 7B), 3 genes that are up-regulated (Figure 7C), and 7 genes that are down-regulated (Figure 7D) upon HSC-activation. Especially the genes that are up-regulated upon HSC activation, being *Ankrd52*, *Clcn5* and *Peg10* are of interest, as miRNAs are known to regulate gene expression in a dominantly negative manner.

miRNA expression analysis in the CCl_4-mouse model

We next analysed the expression of miRNA-451a, miRNA-142-5p, Let-7f-5p, and miRNA-378a-3p in a well-studied mouse model of liver fibrosis, being repeated injections of carbon tetrachloride (CCl_4) (Scholten, Trebicka, Liedtke, & Weiskirchen, 2015). When mice are exposed to the CCl_4-toxin two times a week, for four weeks, significant hepatocyte-damage and HSC-activation can be seen (Figure 8A). Analysis of total liver tissue from sick mice, compared to healthy controls, reveals significant changing levels for miRNA-451a, miRNA-142-5p, Let-7f-5p, and miRNA-378a-3p (Figure 8B), with overlapping expression patterns as found in activating HSCs. Expression of two miRNAs extensively characterized in chronic liver diseases, the hepatocyte-specific miRNA-122-5p (Li et al., 2013) and the HSC-specific miRNA-29a-3p (Roderburg et al., 2011) (Figure 9), were used as positive controls. Plasma obtained from the CCl_4-mouse model identified significant changing expression levels of all analysed miRNAs (Figure 8C). Interestingly, all miRNAs have a plasma expression pattern opposite to what was found in total liver tissue or activating HSCs. Altogether, these results suggest the potential use of these circulating miRNAs, without the need to distinguish between miRNAs packaged into extracellular vesicles or bound to (lipo-)proteins, as markers for HSC activation and fibrosis progression.

Patient characteristics and plasma miRNA alterations during liver fibrosis progression

Next, we investigated whether the plasma levels of these six miRNAs can be correlated to liver fibrosis severity in patients suffering from different chronic liver diseases. Patient characteristics are summarized in Table 9. A total of 208 patients were included, of which 92 patients were diagnosed with no or minimal fibrosis (F0-1) and 116 patients with significant fibrosis ($F \geq 2$), as staged by elastography. Patients with various aetiologies of liver disease were recruited, being chronic alcohol abuse (n = 33), chronic HBV/HCV infection (n = 74) and NAFLD

(n = 101). Patients with chronic alcohol abuse or viral infection underwent transient elastography (FibroScan®) to distinguish significant liver fibrosis (F ≥ 2) from no or minimal fibrosis (F0-1); (median [25th; 75th percentile]) 12 [9.1; 33.6] kPa vs 5.2 [4.0; 6.1] kPa, respectively. Patients who presented with NAFLD, all suffered from Diabetes Mellitus type 2 and underwent ARFI to distinguish significant liver fibrosis (F ≥ 2) from no or minimal fibrosis (F0-1); (median [25th; 75th percentile]) 1.525 [1.30; 1.68] m/s vs 1.15 [1.12; 1.20] m/s, respectively. Various clinical scoring algorithms such as the AST/ALT ratio, Fib-4 score, APRI, and the recently developed PRTA-score (Lambrecht et al., 2019), were calculated. All liver-related laboratory parameters, except for ALT and Creatinine values, and all fibrosis scoring tools are significantly different between the F0-1 and F ≥ 2 patient cohorts, validating the early- or late disease character of the included patients (Table 9).

Analysis of the plasma of these patients showed that miRNA-451a and miRNA-142-5p were significantly up-regulated, while Let-7f-5p was significantly down-regulated, in patients with significant liver fibrosis (F ≥ 2). miRNA-378a-3p remained stable during fibrosis progression (Figure 10A). AUROC analysis identified comparable diagnostic utility among miRNA-451a (AUC = 0.6065), miRNA-142-5p (AUC = 0.6220), and Let-7f-5p (AUC = 0.6485) (Figure 10A and Table 10). Late-stage fibrosis markers miRNA-122-5p (AUC = 0.5969) and miRNA-29a-3p (AUC = 0.5922) (Figure 10B-C and Table 10) were found to have lower diagnostic utility. While APRI (AUC = 0.6481) and AST/ALT (AUC = 0.5956) were comparable to or were outperformed by the analysed miRNAs, FIB-4 (AUC = 0.6879) and the PRTA-score (AUC = 0.7732) remained superior for diagnosis of significant liver fibrosis (Figure 10D and Table 10).

Association of circulating miRNAs with clinical variables

We next examined the association between miRNA expression levels and clinical-pathological variables of the patient cohort. The levels of miRNA-451a (r = -0.2118), miRNA-142-5p (r = -0.2074), Let-7f-5p (r = 0.3426), miRNA-122-5p (r = 0.2193), and miRNA-29a-3p (r = 0.2413) were correlated to fibrosis-severity, as determined by elastography (Table 11 and Figure 11). Let-7f-5p was correlated to various fibrosis-linked parameters, such as decreasing albumin levels (r = -0.2031) and platelet counts (r = -0.3778), and to the fibrosis-scores Fib-4 (r = 0.3215), APRI (r = 0.2820), and PRTA-score (r = 0.4332), suggesting its association to hepatic fibrosis severity. As expected, miRNA-122-5p was strongly associated to AST (r = -0.2625) and ALT (r = -0.4093) levels, and thus marks hepatocyte damage. miRNA-142-5p (r = -0.1602), Let-7f-5p (r = 0.1416), and miRNA-122-5p (r = 0.2628) were associated to age, while Let-7f-5p (r = -0.1563) and miRNA-29a-3p (r =-0.2161) were associated to body mass index (Table 12).

Discrimination of significant liver fibrosis by the miRFIB-score

To investigate whether a combination of the evaluated miRNAs could be used to diagnosis significant (F ≥ 2) liver fibrosis with a higher predictive value than the individual miRNAs, we created a miRNA-algorithm using logistic regression analysis. Hereto, the total patient cohort (n = 208) was randomly divided (Excel, Microsoft, WA, USA) into a derivation (n = 143) and validation (n = 65) cohort. Considering the lack of association between miRNA-378a-3p and fibrosis severity (Figure 8 and Table 11), we choose to exclude this miRNA from the score. Combination of the other miRNA-variables generated the miRFIB-score:

miRFIB = 4.3799 + (0.70824 x Let-7f-5p (dCT)) - (0.0.90912 x miRNA-122-5p (dCT)) - (0.26149 x miRNA-142-5p (dCT)) - (0.53602 x miRNA-29a-3p (dCT)) - (0.041140 x miRNA-451a (dCT))

The diagnostic value of the miRFIB-score to diagnose significant liver fibrosis in the derivation cohort was superior (AUC = 0.7251) to the clinical scores AST/ALT, APRI, and Fib-4 (AUC of 0.5936, 0.6273, and 0.6773 respectively). The diagnostic value of the miRFIB-score was confirmed in the validation cohort (AUC = 0.8173) and total cohort (AUC = 0.7558) (Table 13 and Figure 12). Additionally, the miRFIB-score was found to be significantly correlated to fibrosis severity (r = 0.4365) (Table 11) and was able to differentiate patients with specific stage F2 from patients with stage F0-1 ($p < 0.0001$) (Figure 11).

Inclusion of PDGFRβ improves the diagnostic power of the miRFIB-score

We previously reported the diagnostic utility of circulating PDGFRβ protein levels to detect significant liver fibrosis (Lambrecht et al., 2019). Thus, we performed logistic regression analysis on the derivation cohort, combining PDGFRβ levels with our five-miRNA panel. This generated the miRFIB^{p}-score which was calculated as follows:

miRFIB^{p} score = (0.97229 x miRFIB-score) + (0.00021150 x PDGFRβ (pg/mL) - 1.8678

The score had an increased diagnostic value for the identification of significant liver fibrosis in the derivation cohort (AUC = 0.7912; sensitivity = 80.82%; specificity = 70.37%), validation cohort (AUC = 0.8009; sensitivity = 68.75%; sensitivity = 81.48%) and total cohort (AUC = 0.7970; sensitivity = 79.05%; sensitivity = 69.51%) (Table 13 and Figure 12). Inclusion of PDGFRβ into the miRFIB-score further improves the correlation to fibrosis severity (r = 0.4847) (Table 11), with persistent possibility to differentiate patients with specific stage F2 liver fibrosis from patients with stage F0-1 fibrosis ($p < 0.0001$) (Figure 11).

Table 9 Baseline characteristics of the patient cohort

Patient cohorts	F0-1	F2-4	p-value
Individuals, n	92	116	
Disease aetiology: n (%)			
Alcoholic liver disease	6 (7%)	27 (23%)	
Viral liver disease	46 (50%)	28 (24%)	
NAFLD	40 (43%)	61 (53%)	
Characteristics			
Age (years): median (IQR)	52 (42-63)	57 (51-65)	0.0003
Male, n (%)	52 (57%)	84 (72%)	0.0267
BMI (kg/m^2): median (IQR)	27.44 (24.16-32.35)	29.96 (25.18-34.23)	ns
Laboratory parameters: median (IQR)			
AST (IU/L)	34 (24-48)	40 (28-67)	0.0048
ALT (IU/L)	43 (34-62)	48 (32-71)	ns
Alk Phos (IU/L)	68 (54-87)	87 (66-130)	< 0.0001
GGT (IU/L)	39 (23-83)	71 (40-154)	< 0.0001
Total bilirubin (mg/dL)	0.60 (0.47-0.79)	0.76 (0.57-1.20)	0.0005
Albumin (g/L)	43 (41-46)	42 (39-45)	0.0035
Thrombocytes (x10^3/mm^3)	231 (202-277)	202 (149-255)	0.0006
Creatinine (mg/dL)	0.85 (0.70-1.02)	0.87 (0.74-1.04)	ns
Fibrosis scoring: median (IQR)			
AST/ALT ratio	0.76 (0.62-0.87)	0.82 (0.67-1.18)	0.0211
APRI	0.35 (0.24-0.57)	0.56 (0.32-0.88)	0.0005
Fib-4	1.13 (0.83-1.49)	1.67 (1.08-2.80)	< 0.0001
PRTA-score	7.18 (4.49-9.87)	11.63 (7.95-20.40)	< 0.0001

n: number; NAFLD: non-alcoholic fatty liver disease; IQR: interquartile range; BMI: body mass index; AST: aspartate aminotransferase; ALT: alanine aminotransferase; Alk Phos: alkaline phosphatase; GGT: gamma-glutamyl transferase; AST/ALT ratio: aspartate aminotransferase/alanine aminotransferase ratio; APRI: AST to platelet ratio index; Fib-4: Fibrosis-4; PRTA-score: PDGFRβ-thrombocytes-albumin score; ns: not significant.

Table 10. Performance of individual plasma miRNAs, as compared to the AST/ALT, APRI, Fib-4, and PRTA scoring algorithms, for the detection of significant liver fibrosis (F ≥ 2).

	AUC	95% CI	Optimal cut-off	Sensitivity (%)	Specificity (%)	PPV	NPV
miRNA-451a	0.6065	0.5282-0.6484	2.224	58.41	62.92	66.50	54.55
miRNA-142-5p	0.6220	0.5445-0.6994	7.653	43.75	85.23	78.87	54.59
Let-7f-5p	0.6485	0.5739-0.7231	3.292	56.90	76.09	74.99	58.35
miRNA-378a-3p	0.5176	0.4389-0.5962	10.27	23.48	91.30	77.28	48.63
miRNA-122-5p	0.5969	0.5195-0.6744	7.102	46.55	72.22	67.87	51.74
miRNA-29a-3p	0.5922	0.5147-0.6698	7.399	29.82	95.60	89.52	51.94
Fib-4	0.6879	0.6112-0.7647	1.505	60.19	77.50	77.13	60.70
APRI	0.6481	0.5696-0.7267	0.4928	57.01	70.37	70.80	56.49
AST/ALT	0.5956	0.5166-0.6746	0.8725	41.82	75.86	68.59	50.85
PRTA-score	0.7732	0.7033-0.8431	11.59	50.52	89.71	86.09	58.99

Table 11. Correlation of circulating miRNA expression levels with fibrosis stage.
Correlations were evaluated by the Pearson's correlation coefficient (r). ns: not significant.

	Correlation to F-score	
	r	*p*
miRNA-451a	-0.2118	0.0025
miRNA-142-5p	-0.2074	0.0032
Let-7f-5p	0.3426	< 0.0001
miRNA-378a-3p	-0.0119	ns
miRNA-122-5p	0.2193	0.0015
miRNA-29a-3p	0.2413	0.0005
miRFIB	0.4365	< 0.0001
miRFIB^P	0.4847	< 0.0001

Table 12. Correlation of circulating miRNA expression levels with clinical parameters.

	miRNA-451a		miRNA-142-5p		Let-7f-5p		miRNA-378a-3p		miRNA-122-5p		miRNA-29a-3p	
	r	*p*	*r*	*p*	*r*	*p*	*r*	*p*	*r*	*p*	*r*	*p*
Age	-0.0409	ns	-0.1602	0.0234	0.1416	0.0413	0.0905	ns	0.2628	0.0001	0.0096	ns
BMI	0.0280	ns	-0.0397	ns	-0.1563	0.0287	-0.1037	ns	-0.0667	ns	-0.2161	0.0025
AST	-0.1554	0.0318	0.0076	ns	0.1371	ns	-0.1038	ns	-0.2625	0.0002	0.1150	ns
ALT	-0.0727	ns	0.0207	ns	0.0534	ns	-0.1412	0.0484	-0.4093	< 0.0001	-0.0166	ns
Alk Phos	-0.0022	ns	-0.0804	ns	0.2027	0.0050	-0.0047	ns	0.2059	0.0046	0.1600	0.0287
GGT	-0.1372	ns	-0.1756	0.0174	0.1730	0.0163	-0.0621	ns	0.0060	ns	0.0899	ns
Bilirubin	-0.0609	ns	-0.0237	ns	0.3194	< 0.0001	0.1295	ns	0.1213	ns	0.2790	0.0001
Albumin	-0.1064	ns	0.0365	ns	-0.2031	0.0067	-0.0148	ns	-0.2394	0.0014	-0.1747	0.0207
Platelet count	0.1243	ns	-0.1139	ns	-0.3778	< 0.0001	-0.1629	0.0255	-0.1050	ns	-0.3514	< 0.0001
Creatinine	-0.0419	ns	-0.0399	ns	0.0054	ns	-0.0094	ns	0.0652	ns	-0.0257	ns
AST/ALT	-0.1026	ns	-0.0126	ns	0.0756	ns	0.0311	ns	0.1920	0.0072	0.1627	0.0234
Fib-4	-0.1223	ns	0.0439	ns	0.3215	< 0.0001	0.1400	ns	0.0607	ns	0.2852	0.0001
APRI	-0.1551	0.0365	0.1039	ns	0.2820	< 0.0001	0.0321	ns	-0.1573	0.0321	0.2551	0.0005
PRTA-score	-0.0559	ns	0.0266	ns	0.4332	< 0.0001	0.1479	ns	0.2401	0.0020	0.3447	< 0.0001

Table 13. Performance of the miRFIB- and miRFIBp score, as compared to the AS/ALT, APRI, Fib-4, and PRTA score algorithms, for the detection of significant liver fibrosis (F ≥ 2).

	AUC	95% CI	Optimal cut-off	Sensitivity (%)	Specificity (%)	PPV	NPV
AST/ALT							
Derivation	0.5936	0.4986-0.6886	0.6948	73.68	45.16	62.87	58.65
Validation	0.5988	0.4546-0.7430	1.025	38.24	84.00	75.08	51.90
Total	0.5956	0.5166-0.6747	0.8725	41.82	75.86	68.59	50.85
APRI							
Derivation	0.6273	0.5313-0.7234	0.4928	59.46	68.97	70.72	57.44
Validation	0.7128	0.5773-0.8482	0.7531	45.45	95.65	92.94	58.18
Total	0.6481	0.5696-0.7267	0.4928	57.01	70.37	70.80	56.49
Fib-4							
Derivation	0.6773	0.5847-0.7698	1.505	61.11	73.68	74.53	60.05
Validation	0.7083	0.5692-0.8474	1.520	58.06	86.96	84.88	62.19
Total	0.6879	0.6112-0.7647	1.505	60.19	77.50	77.13	60.70
PRTA-score							
Derivation	0.7399	0.6525-0.8272	10.36	59.15	81.63	80.23	61.32
Validation	0.7912	0.6566-0.9258	7.842	86.21	72.22	79.64	80.60
Total	0.7732	0.7033-0.8431	11.59	50.52	89.71	86.09	58.99
miRFIB							
Derivation	0.7251	0.6393-0.8110	0.1109	77.33	61.40	71.63	68.24
Validation	0.8173	0.7112-0.9235	0.3412	65.71	92.86	92.06	68.24
Total	0.7558	0.6887-0.8229	0.1404	78.38	62.35	72.41	69.59
miRFIB^{p}							
Derivation	0.7912	0.7120-0.8704	0.0673	80.82	70.37	77.47	74.43
Validation	0.8009	0.6844-0.9175	0.3840	68.75	81.48	82.39	67.41
Total	0.7970	0.7329-0.8611	0.1043	79.05	69.51	76.57	72.47

REFERENCES.

Cao, S., Yaqoob, U., Das, A., Shergill, U., Jagavelu, K., Huebert, R. C., . . . Shah, V. H. (2010). Neuropilin-1 promotes cirrhosis of the rodent and human liver by enhancing PDGF/TGF-beta signaling in hepatic stellate cells. *J Clin Invest, 120*(7), 2379-2394. doi:10.1172/JCI41203

Dekervel, J., Bulle, A., Windmolders, P., Lambrechts, D., Van Cutsem, E., Verslype, C., & van Pelt, J. (2017). Acriflavine Inhibits Acquired Drug Resistance by Blocking the Epithelial-to-Mesenchymal Transition and the Unfolded Protein Response. *Transl Oncol, 10*(1), 59-69. doi:10.1016/j.tranon.2016.11.008

Foucher, J., Castera, L., Bernard, P. H., Adhoute, X., Laharie, D., Bertet, J., . . . de Ledinghen, V. (2006). Prevalence and factors associated with failure of liver stiffness measurement using FibroScan in a prospective study of 2114 examinations. *Eur J Gastroenterol Hepatol, 18*(4), 411-412.

Friedrich-Rust, M., Ong, M. F., Martens, S., Sarrazin, C., Bojunga, J., Zeuzem, S., & Herrmann, E. (2008). Performance of transient elastography for the staging of liver fibrosis: a meta-analysis. *Gastroenterology, 134*(4), 960-974. doi:10.1053/j.gastro.2008.01.034

Guimaraes, E. L., Empsen, C., Geerts, A., & van Grunsven, L. A. (2010). Advanced glycation end products induce production of reactive oxygen species via the activation of NADPH oxidase in murine hepatic stellate cells. *J Hepatol, 52*(3), 389-397. doi:10.1016/j.jhep.2009.12.007

Lambrecht, J., Jan Poortmans, P., Verhulst, S., Reynaert, H., Mannaerts, I., & van Grunsven, L. A. (2017). Circulating ECV-Associated miRNAs as Potential Clinical Biomarkers in Early Stage HBV and HCV Induced Liver Fibrosis. *Front Pharmacol, 8*, 56. doi:10.3389/fphar.2017.00056

Lambrecht, J., Verhulst, S., Mannaerts, I., Reynaert, H., & van Grunsven, L. A. (2018). Prospects in non-invasive assessment of liver fibrosis: Liquid biopsy as the future gold standard? *Biochim Biophys Acta, 1864*(4 Pt A), 1024-1036. doi:10.1016/j.bbadis.2018.01.009

Lambrecht, J., Verhulst, S., Mannaerts, I., Sowa, J. P., Best, J., Canbay, A., . . . van Grunsven, L. A. (2019). A PDGFRbeta-based score predicts significant liver fibrosis in patients with chronic alcohol abuse, NAFLD and viral liver disease. *EBioMedicine, 43*, 501-512. doi:10.1016/j.ebiom.2019.04.036

Li, J., Ghazwani, M., Zhang, Y., Lu, J., Li, J., Fan, J., . . . Li, S. (2013). miR-122 regulates collagen production via targeting hepatic stellate cells and suppressing P4HA1 expression. *J Hepatol, 58*(3), 522-528. doi:10.1016/j.jhep.2012.11.011

Pinzani, M., Milani, S., Herbst, H., DeFranco, R., Grappone, C., Gentilini, A., . . . Gentilini, P. (1996). Expression of platelet-derived growth factor and its receptors in normal human liver and during active hepatic fibrogenesis. *Am J Pathol, 148*(3), 785-800.

Raposo, G., & Stoorvogel, W. (2013). Extracellular vesicles: exosomes, microvesicles, and friends. *J Cell Biol, 200*(4), 373-383. doi:10.1083/jcb.201211138

Roderburg, C., Urban, G. W., Bettermann, K., Vucur, M., Zimmermann, H., Schmidt, S., . . . Luedde, T. (2011). Micro-RNA profiling reveals a role for miR-29 in human and murine liver fibrosis. *Hepatology, 53*(1), 209-218. doi:10.1002/hep.23922

Sandrin, L., Fourquet, B., Hasquenoph, J. M., Yon, S., Fournier, C., Mal, F., . . . Palau, R. (2003). Transient elastography: a new noninvasive method for assessment of hepatic fibrosis. *Ultrasound Med Biol, 29*(12), 1705-1713.

Schindelin, J., Arganda-Carreras, I., Frise, E., Kaynig, V., Longair, M., Pietzsch, T., . . . Cardona, A. (2012). Fiji: an open-source platform for biological-image analysis. *Nat Methods, 9*(7), 676-682. doi:10.1038/nmeth.2019

Scholten, D., Trebicka, J., Liedtke, C., & Weiskirchen, R. (2015). The carbon tetrachloride model in mice. *Lab Anim, 49*(1 Suppl), 4-11. doi:10.1177/0023677215571192

Seger, S., Stritt, M., Vezzali, E., Nayler, O., Hess, P., Groenen, P. M. A., & Stalder, A. K. (2018). A fully automated image analysis method to quantify lung fibrosis in the bleomycin-induced rat model. *PLoS One, 13*(3), e0193057. doi:10.1371/journal.pone.0193057

Starkel, P., & Leclercq, I. A. (2011). Animal models for the study of hepatic fibrosis. *Best Pract Res Clin Gastroenterol, 25*(2), 319-333. doi:10.1016/j.bpg.2011.02.004

Stradiot, L., Verhulst, S., Roosens, T., Oie, C. I., Moya, I. M., Halder, G., . . . van Grunsven, L. A. (2017). Functionality based method for simultaneous isolation of rodent hepatic sinusoidal cells. *Biomaterials, 139*, 91-101. doi:10.1016/j.biomaterials.2017.05.047

Thery, C., Amigorena, S., Raposo, G., & Clayton, A. (2006). Isolation and characterization of exosomes from cell culture supernatants and biological fluids. *Curr Protoc Cell Biol, Chapter 3*, Unit 3 22. doi:10.1002/0471143030.cb0322s30

Youden, W. J. (1950). Index for rating diagnostic tests. *Cancer, 3*(1), 32-35.

CLAIMS

1. An *in vitro* method of diagnosing fibrosis in a subject, said method comprising:
a) determining the level of soluble PDGFRβ (sPDGFRβ) in a biological fluid test sample obtained from said subject; and
b) comparing said level of sPDGFRβ to a reference level of sPDGFRβ that is characteristic of a healthy subject without fibrosis in order to diagnose whether the subject has fibrosis,
wherein an increase in sPDGFRβ in the test sample compared to the reference level is indicative for fibrosis.

2. An *in vitro* method of diagnosing the severity of fibrosis in a subject, said method comprising:
a) determining the level of sPDGFRβ in a biological fluid test sample obtained from said subject; and
b) comparing said level of sPDGFRβ to a predetermined level of said sPDGFRβ in a population of subjects ranging from no fibrosis to severe fibrosis.

3. An *in vitro* method of determining the prognosis of fibrosis in a subject, said method comprising:
a) determining the level of sPDGFRβ in a biological fluid test sample obtained from said subject; and
b) comparing said level of sPDGFRβ to a reference level of sPDGFRβ that is characteristic of a healthy subject without fibrosis in order to determine the prognosis of fibrosis in said subject,
wherein an increase in sPDGFRβ in the test sample compared to the reference level is indicative for the prognosis of the subject.

4. An *in vitro* method of assessing the efficacy of a therapeutic agent against fibrosis in a subject, said method comprising
a) determining the level of soluble PDGFRβ (sPDGFRβ) in a first biological fluid test sample obtained from said subject wherein said first biological test sample is obtained at a time point before the start of the treatment;
b) determining the level of sPDGFRβ in one or more subsequent biological fluid test samples obtained from said subject wherein said one or more subsequent biological test samples are obtained at regular intervals after the start of the treatment;
c) comparing the level of sPDGFRβ in the first biological fluid test sample with the level of sPDGFRβ in the one or more subsequent biological fluid test samples in order to assess the efficacy of the therapeutic agent;
wherein a decrease in the level of sPDGFRβ in the one or more subsequent test samples as compared to the level of sPDGFRβ in the first test sample is indicative for a decrease in disease

progression in the subject, and

wherein an increase in the level of sPDGFRβ in the one or more subsequent test samples as compared to the level of sPDGFRβ in the first test sample is indicative for an increase in disease progression in the subject.

5. The *in vitro* method according to any one of claims 1 to 4, wherein the biological fluid test sample is further analyzed to determine the level(s) of one or more additional biomarkers for fibrosis and wherein the level(s) of said one or more additional biomarkers are compared to the reference levels of said one or more additional biomarkers that are characteristic of a healthy subject without fibrosis in order to diagnose the presence or severity of fibrosis or in order to determine the prognosis of fibrosis in said subject.

6. The *in vitro* method according to claim 5, wherein said one or more biomarkers are selected from the group comprising aspartate transaminase (AST), alanine transaminase (ALT) , alkaline phosphatase, bilirubin, albumin, gamma-glutamyl transferase, creatinine, alpha-fetoprotein, the thrombocyte level, and the level of one or more circulating miRNAs; in particular albumin, thrombocyte level and the level of one or more circulating miRNAs.

7. The *in vitro* method according to claim 6, wherein the biological fluid test sample is further analyzed to determine the albumin and thrombocyte levels, and wherein the albumin and thrombocyte levels are compared to the reference levels of albumin and thrombocytes that are characteristic of a healthy subject without fibrosis in order to diagnose the presence of severity of fibrosis or in order to determine the prognosis of fibrosis in said subject.

8. The *in vitro* method according to claim 6, wherein the biological fluid test sample is further analysed to determine the level of at least one circulating miRNA; preferably at least five circulating miRNAs.

9. An *in vitro* method of diagnosing the presence and/or severity of fibrosis in a subject, said method comprising calculating the PRTA score, and comparing the PRTA score of said subject to the PRTA score of a healthy subject without fibrosis, wherein the PRTA score is calculated using the formula:

[sPDGFRβ (pg/mL) *100]/ [albumin (g/L) * (thrombocytes (/mm^3)/100)],

and wherein the levels of sPDGFRβ, albumin and thrombocytes are determined in a biological fluid test sample obtained from the subject.

10. An *in vitro* method of determining the prognosis of fibrosis in a subject, said method comprising: calculating the PRTA score, and comparing the PRTA score of said subject to the

PRTA score of a healthy subject without fibrosis, wherein the PRTA score is calculated using the formula:

[sPDGFRβ (pg/mL) *100]/ [albumin (g/L) * (thrombocytes (/mm^3)/100)],

wherein the levels of sPDGFRβ, albumin and thrombocytes are determined in a biological fluid test sample obtained from the subject, and

wherein an increase in PRTA score in the biological fluid test sample compared to the reference level is indicative for the prognosis of the subject.

11. An *in vitro* method of assessing the efficacy of a therapeutic agent against fibrosis in a subject, said method comprising:

a) calculating the PRTA score of said subject at a first time point before the start of the treatment,

b) calculating the PRTA score of said subject at one or more second time points at regular intervals after the start of the treatment,

c) comparing the PRTA score of the first time point with the PRTA score of the one or more second time points in order to assess the efficacy of the therapeutic agent,

wherein the PRTA score is calculated using the formula:

[sPDGFRβ (pg/mL) *100]/ [albumin (g/L) * (thrombocytes (/mm^3)/100)],

wherein the levels of sPDGFRβ, albumin and thrombocytes are determined in a biological fluid test sample obtained from the subject,

wherein a decrease of the PRTA score of the one or more second time points as compared to the PRTA score of the first time point is indicative for a decrease in disease progression in the subject, and

wherein an increase of the PRTA score of the one or more second time points as compared to the PRTA score of the first time point is indicative for an increase in disease progression in the subject.

12. The *in vitro* method according to any one of claims 9 to 11 further comprising determining the levels of at least one circulating miRNA in the biological test sample obtained from the subject; preferably at least five circulating miRNAs in the biological test sample obtained from the subject.

13. The *in vitro* method according to any one of claims 6, 8, or 12, wherein the circulating miRNAs are selected from miRNA-451a, miRNA-142-5p, Let-7f-5p, miRNA-378-3p, miRNA-122-5p, and miRNA-29a-3p; preferably selected from miRNA-451a, miRNA-142-5p, Let-7f-5p, miRNA-122-5p and miRNA-29a-3p.

14. The *in vitro* method according to claim 13 wherein an miRFIB-score is calculated using the following formula:

miRFIB score = 4.3799 + (0.70824 x Let-7F-5p (dCT)) – (0.090912 x miRNA-122-5-p (dCT)) – (0.26149 x miRNA-142-5p (dCT)) – (0.53602 x miRNA-29a-3p (dCT)) – (0.041140 x miRNA-451a (dCT)),
wherein dCT represents the delta CT value of each specific miRNA determined using real-time PCR.

15. The *in vitro* method of claim 14 wherein an miRFIB^{p}-score is calculated using the following formula:
miRFIB^{p}-score = (0.97229 x miRFIBscore) + (0.00021150 x PDGFRβ (pg/ml)) - 1.8678.

16. The *in vitro* method according to any one of claims 1 to 15, wherein fibrosis is selected from the group comprising liver fibrosis, lung fibrosis, kidney fibrosis.

17. The in vitro method according to claim 15 wherein fibrosis is liver fibrosis.

18. The *in vitro* method according to any one of claims 1 to 17, wherein the biological fluid sample comprises blood, plasma, serum, saliva, or urine.

19. The in vitro method according to claim 18, wherein the biological fluid sample comprises blood, plasma or serum.

20. The in vitro method according to any one of the preceding claims, wherein the subject is a human.

Fig. 1

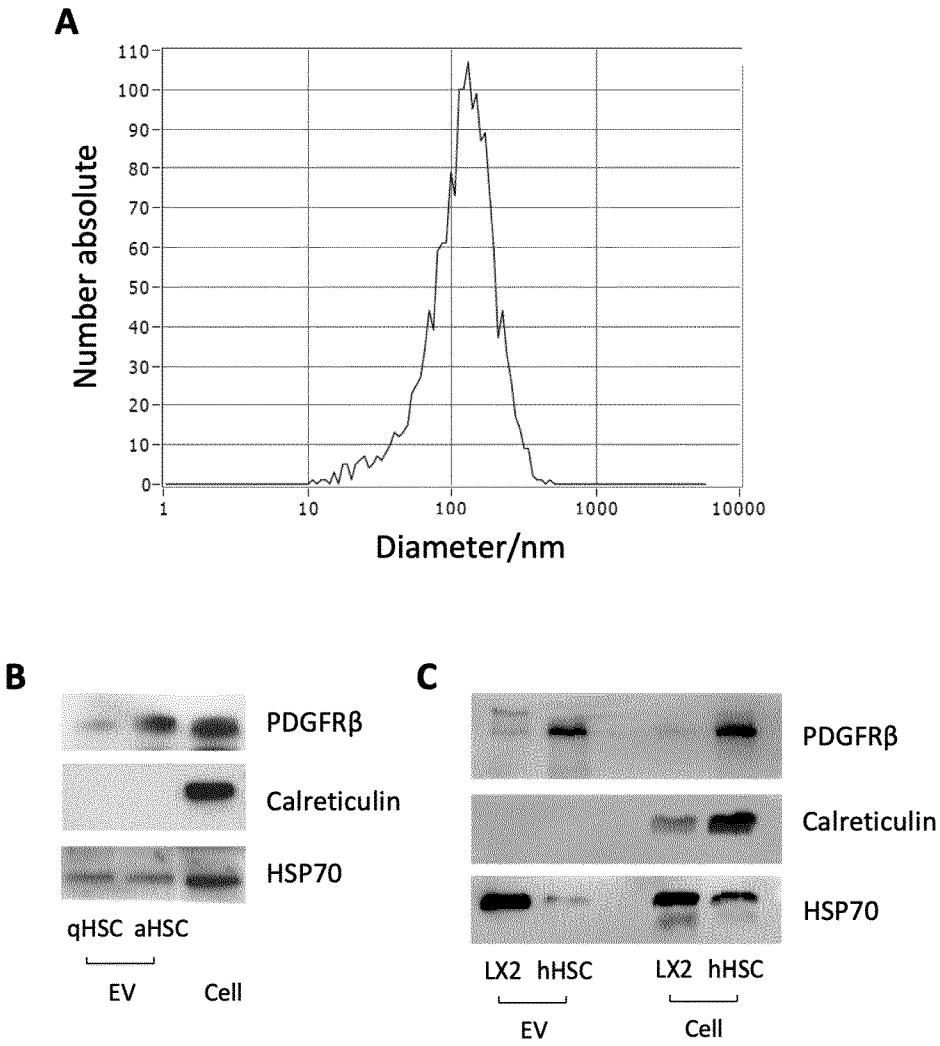

A
Number absolute
110
100
90
80
70
60
50
40
30
20
10
0
1
10
100
1000
10000
Diameter/nm
B
PDGFRβ
Calreticulin
HSP70
qHSC aHSC
EV
Cell
C
PDGFRβ
Calreticulin
HSP70
LX2 hHSC
LX2 hHSC
EV
Cell

Fig. 2

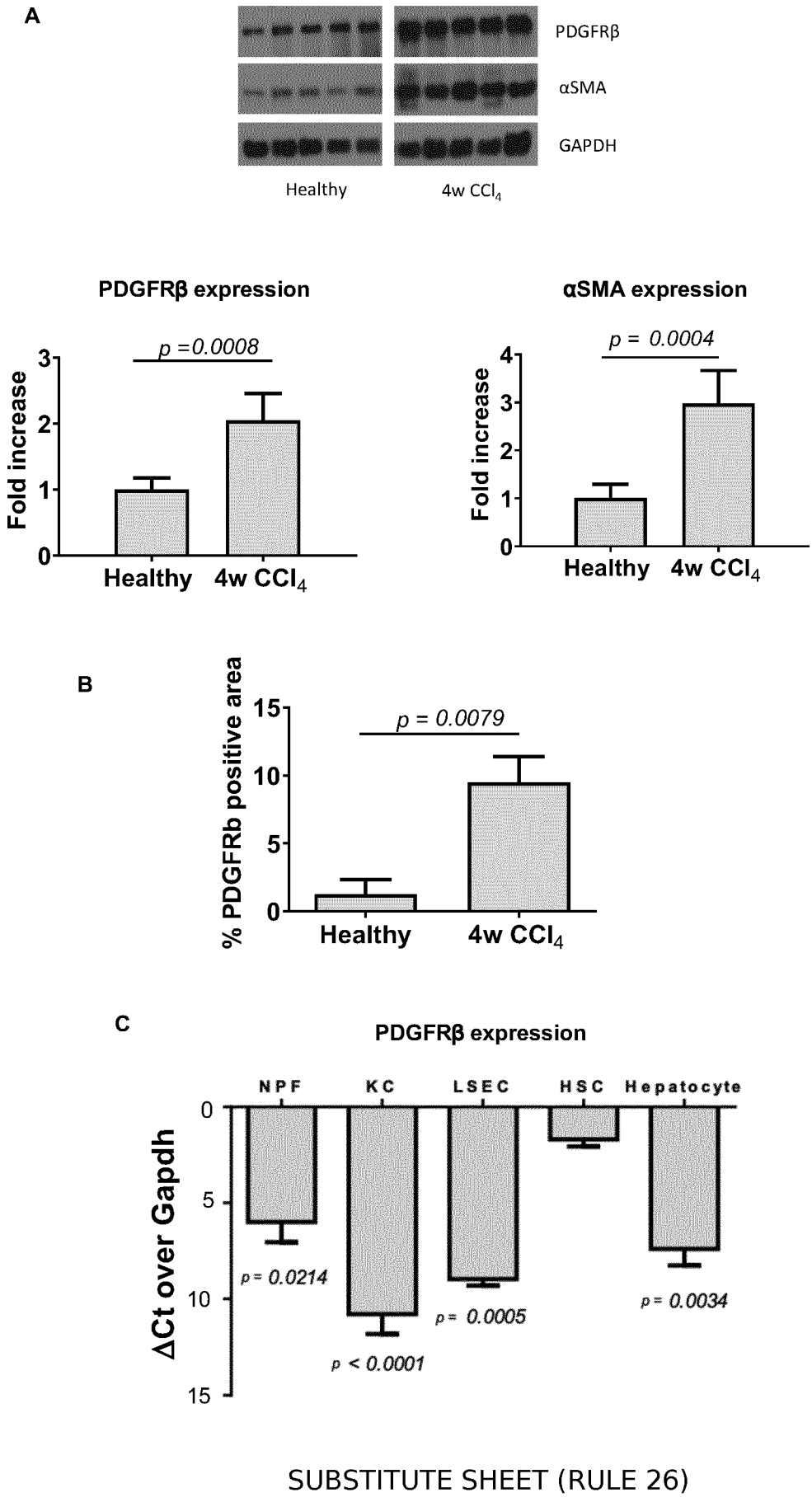
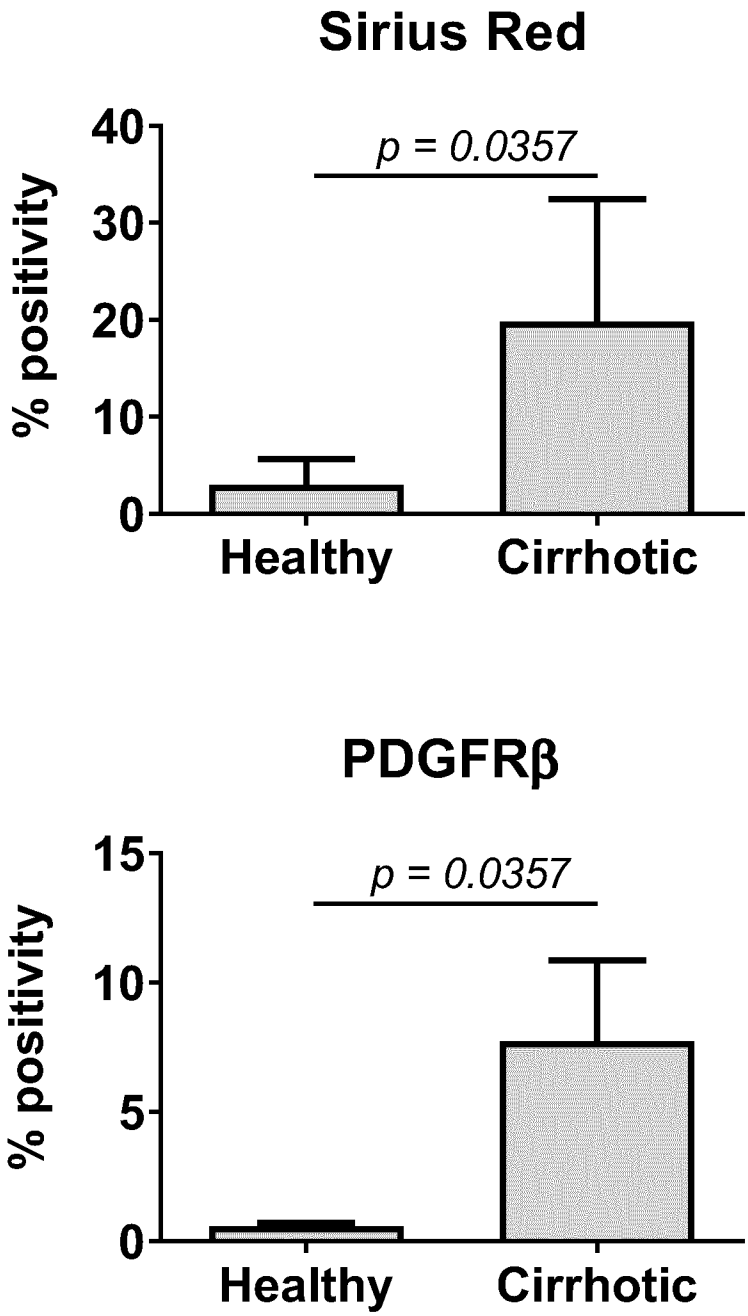

A
PDGFRβ
αSMA
GAPDH
Healthy
4w CCl4
PDGFRβ expression
p =0.0008
Fold increase
Healthy
4w CCl4
αSMA expression
p = 0.0004
Fold increase
Healthy
4w CCl4
B
% PDGFRb positive area
p = 0.0079
Healthy
4w CCl4
C
PDGFRβ expression
NPF
KC
LSEC
HSC
Hepatocyte
ΔCt over Gapdh
p = 0.0214
p < 0.0001
p = 0.0005
p = 0.0034

Fig. 3


Sirius Red
% positivity
40
30
20
10
0
p = 0.0357
Healthy
Cirrhotic
PDGFRβ
% positivity
15
10
5
0
p = 0.0357
Healthy
Cirrhotic

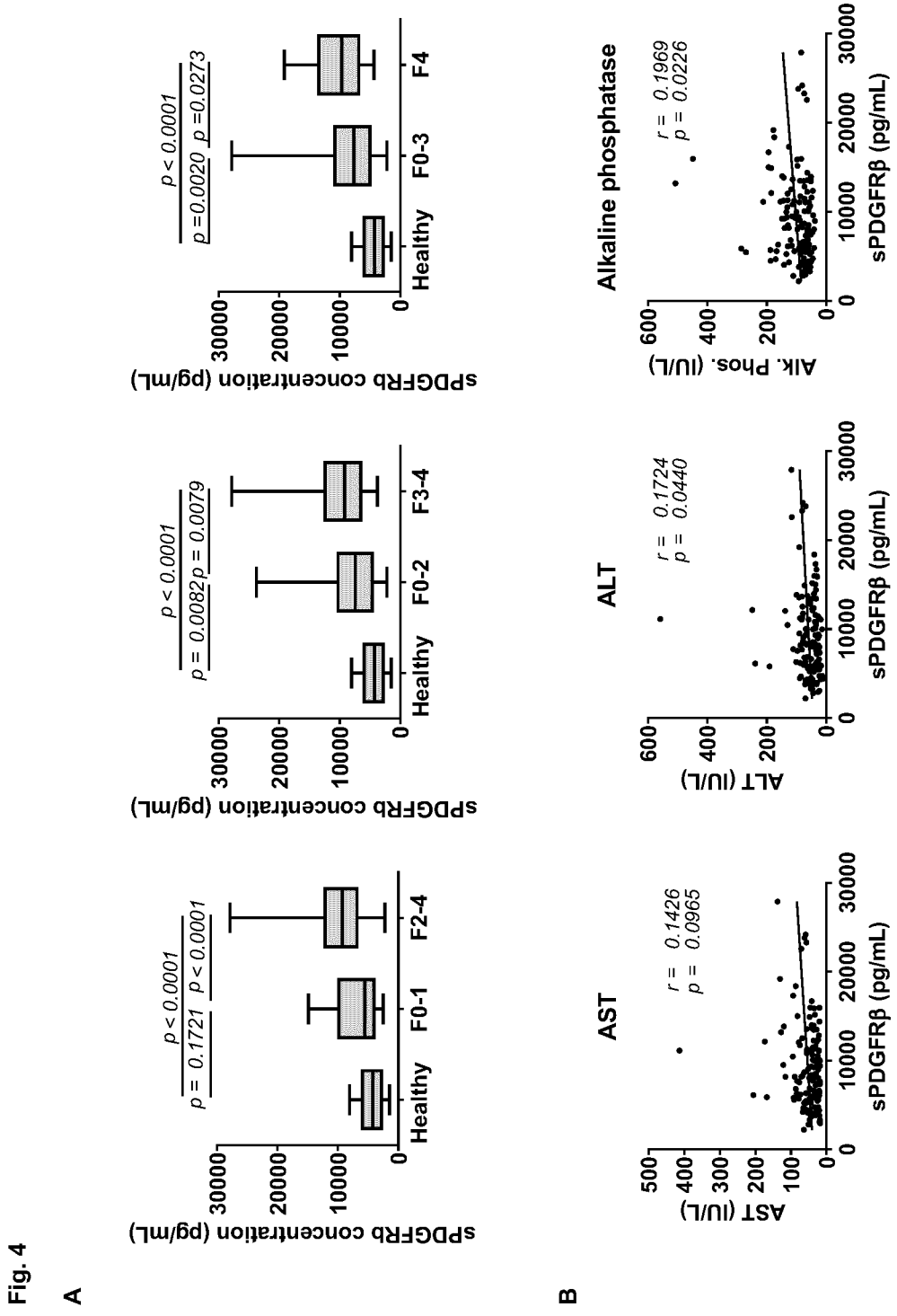

A
sPDGFRb concentration (pg/mL)
30000
20000
10000
0
p < 0.0001
p = 0.1721
p < 0.0001
Healthy
F0-1
F2-4
p < 0.0001
p = 0.0082
p = 0.0079
Healthy
F0-2
F3-4
p < 0.0001
p =0.0020
p =0.0273
Healthy
F0-3
F4
B
AST
AST (IU/L)
500
400
300
200
100
0
r = 0.1426
p = 0.0965
0
10000
20000
30000
sPDGFRβ (pg/mL)
ALT
ALT (IU/L)
600
400
200
0
r = 0.1724
p = 0.0440
0
10000
20000
30000
sPDGFRβ (pg/mL)
Alkaline phosphatase
Alk. Phos. (IU/L)
600
400
200
0
r = 0.1969
p = 0.0226
0
10000
20000
30000
sPDGFRβ (pg/mL)

Fig. 4

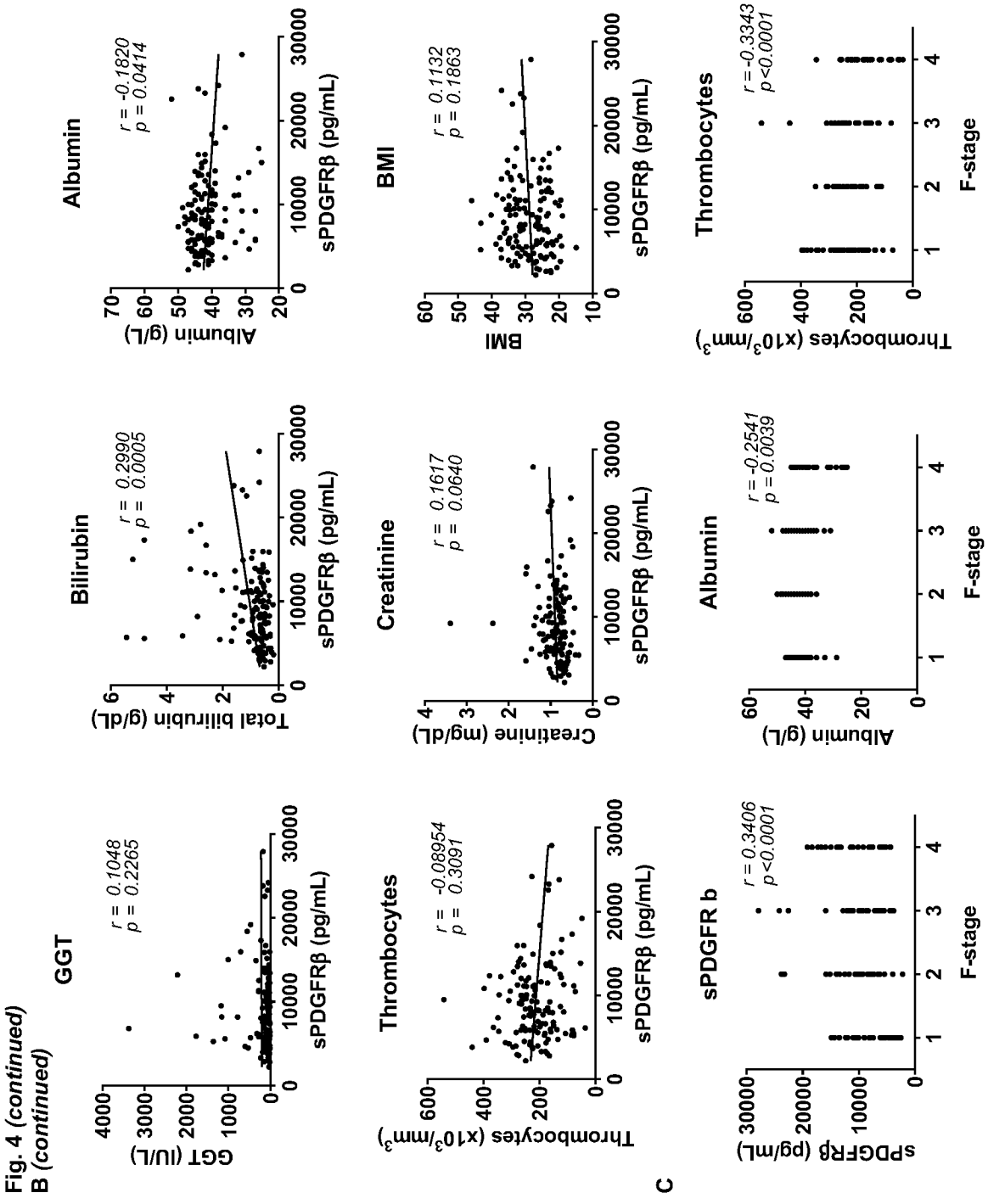

Fig. 4 (continued)
B (continued)
GGT
r = 0.1048
p = 0.2265
GGT (IU/L)
sPDGFRβ (pg/mL)
Bilirubin
r = 0.2990
p = 0.0005
Total bilirubin (g/dL)
sPDGFRβ (pg/mL)
Albumin
r = -0.1820
p = 0.0414
Albumin (g/L)
sPDGFRβ (pg/mL)
Thrombocytes
r = -0.08954
p = 0.3091
Thrombocytes (x10³/mm³)
sPDGFRβ (pg/mL)
Creatinine
r = 0.1617
p = 0.0640
Creatinine (mg/dL)
sPDGFRβ (pg/mL)
BMI
r = 0.1132
p = 0.1863
BMI
sPDGFRβ (pg/mL)
C
sPDGFR b
r = 0.3406
p<0.0001
sPDGFRβ (pg/mL)
F-stage
Albumin
r = -0.2541
p = 0.0039
Albumin (g/L)
F-stage
Thrombocytes
r = -0.3343
p<0.0001
Thrombocytes (x10³/mm³)
F-stage

Fig. 5

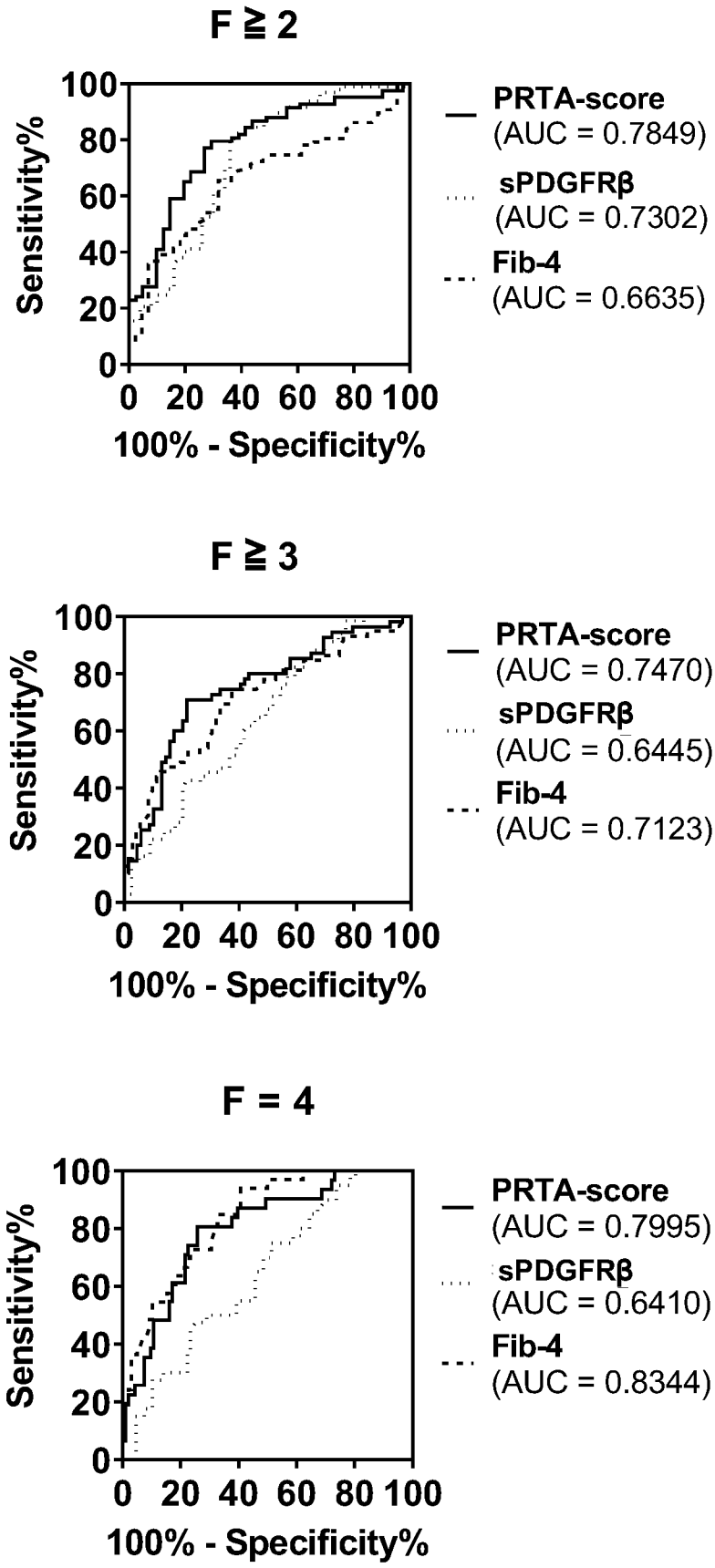
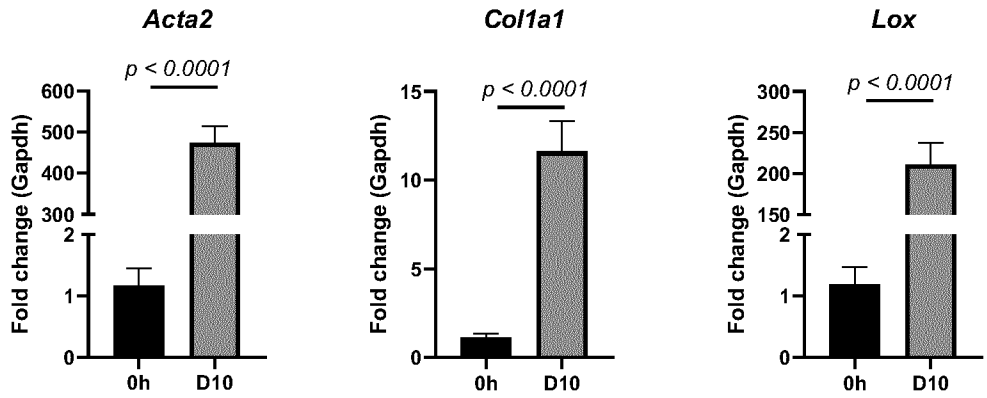

F ≧ 2
Sensitivity%
100% - Specificity%
0 20 40 60 80 100
PRTA-score
(AUC = 0.7849)
sPDGFRβ
(AUC = 0.7302)
Fib-4
(AUC = 0.6635)
F ≧ 3
Sensitivity%
100% - Specificity%
0 20 40 60 80 100
PRTA-score
(AUC = 0.7470)
sPDGFRβ
(AUC = 0.6445)
Fib-4
(AUC = 0.7123)
F = 4
Sensitivity%
100% - Specificity%
0 20 40 60 80 100
PRTA-score
(AUC = 0.7995)
sPDGFRβ
(AUC = 0.6410)
Fib-4
(AUC = 0.8344)

Fig. 6

A


Acta2
p < 0.0001
Fold change (Gapdh)
600
500
400
300
2
1
0
0h
D10
Col1a1
p < 0.0001
Fold change (Gapdh)
15
10
5
0
0h
D10
Lox
p < 0.0001
Fold change (Gapdh)
300
250
200
150
2
1
0
0h
D10

B

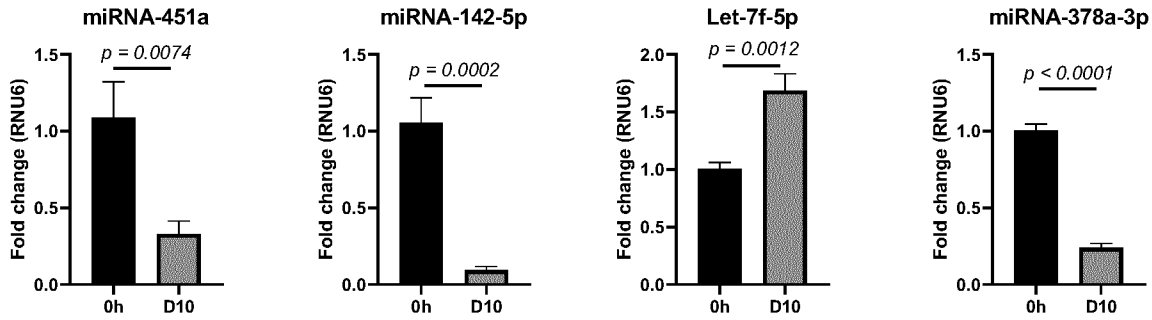
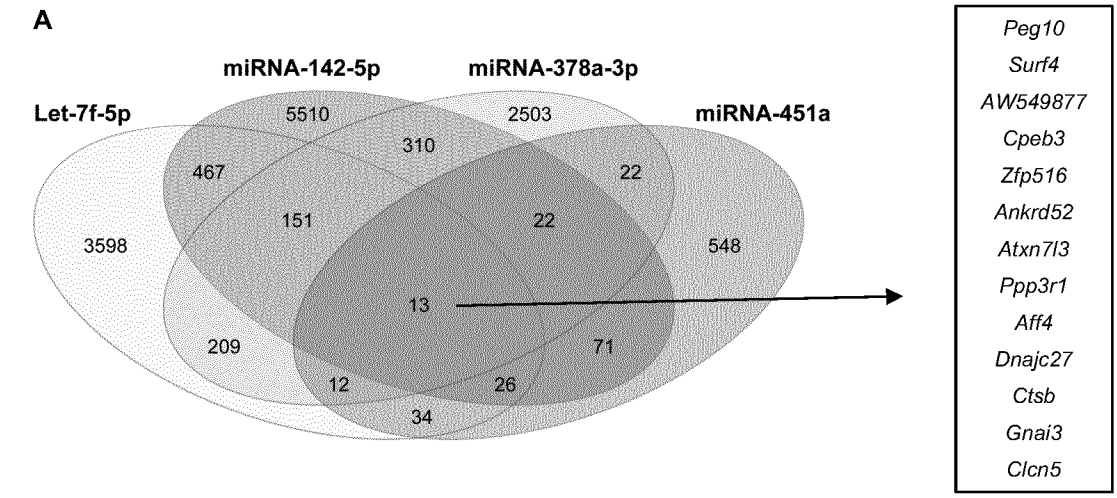
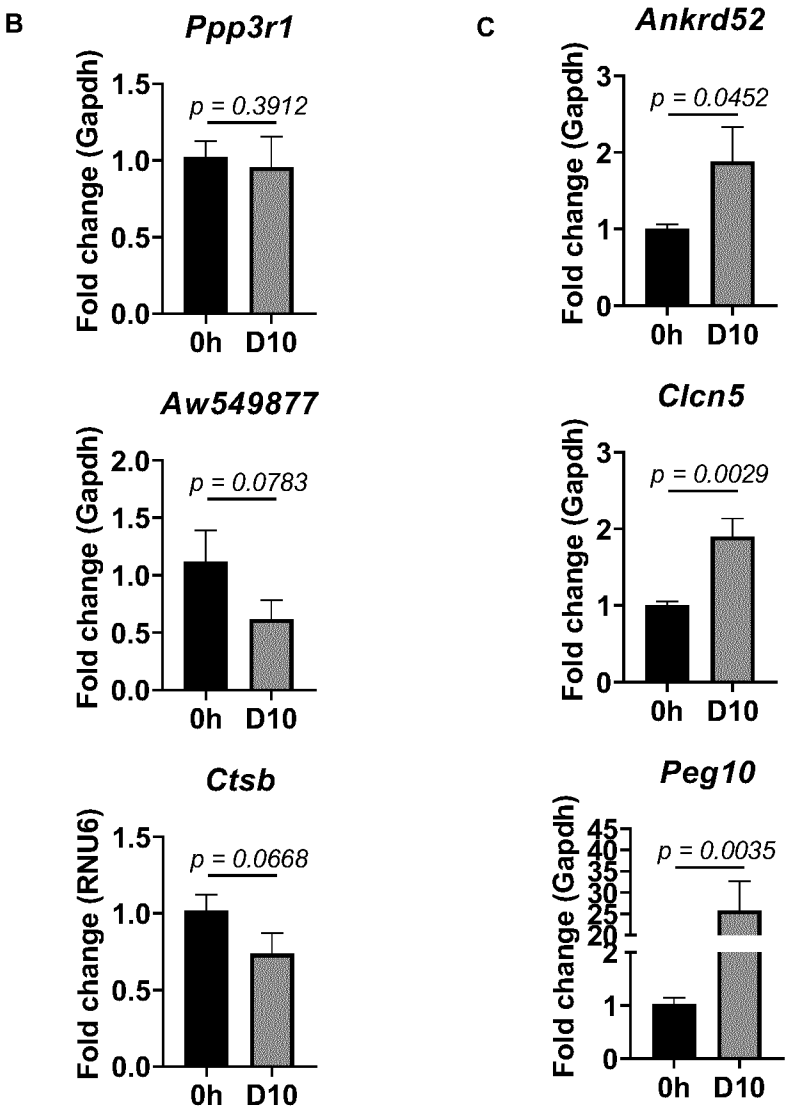

miRNA-451a
p = 0.0074
Fold change (RNU6)
1.5
1.0
0.5
0.0
0h
D10
miRNA-142-5p
p = 0.0002
Fold change (RNU6)
1.5
1.0
0.5
0.0
0h
D10
Let-7f-5p
p = 0.0012
Fold change (RNU6)
2.0
1.5
1.0
0.5
0.0
0h
D10
miRNA-378a-3p
p < 0.0001
Fold change (RNU6)
1.5
1.0
0.5
0.0
0h
D10

Fig. 7


A
miRNA-142-5p
miRNA-378a-3p
Let-7f-5p
miRNA-451a
5510
2503
310
467
22
151
22
3598
548
13
209
71
12
26
34
Peg10
Surf4
AW549877
Cpeb3
Zfp516
Ankrd52
Atxn7l3
Ppp3r1
Aff4
Dnajc27
Ctsb
Gnai3
Clcn5


B
Ppp3r1
Fold change (Gapdh)
p = 0.3912
0h
D10
Aw549877
p = 0.0783
Ctsb
Fold change (RNU6)
p = 0.0668
C
Ankrd52
p = 0.0452
Clcn5
p = 0.0029
Peg10
p = 0.0035

D

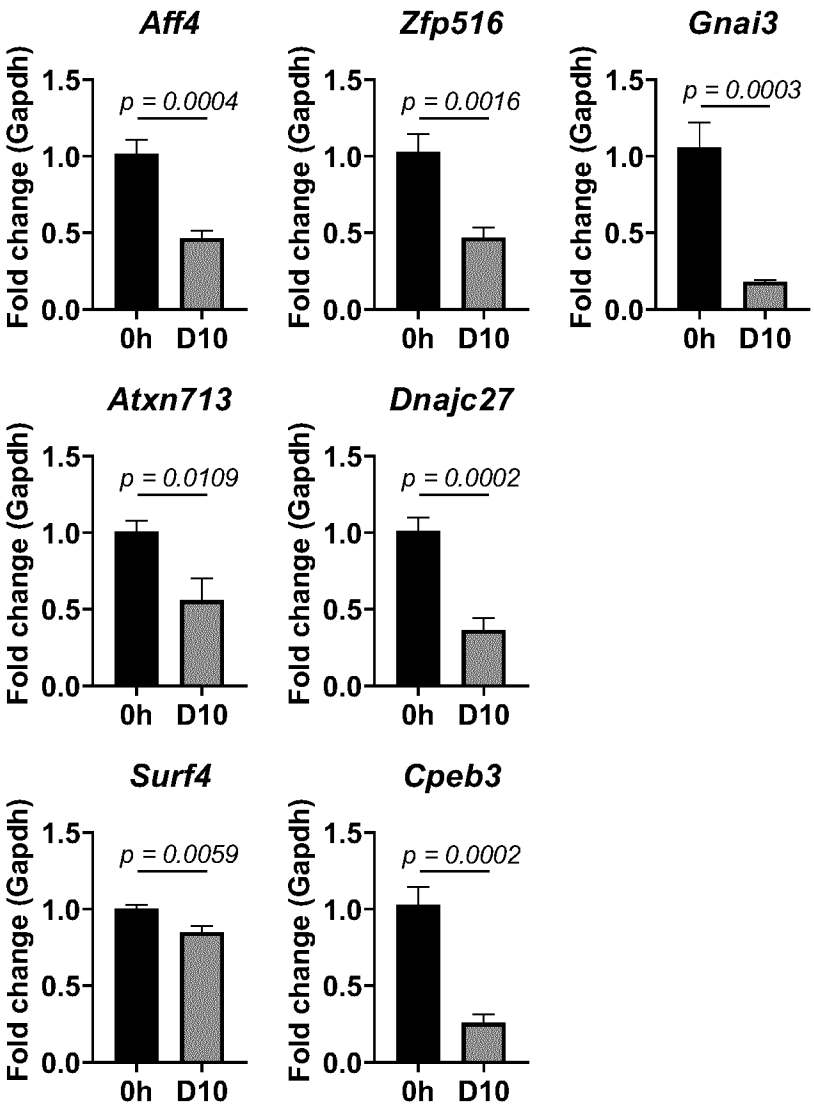
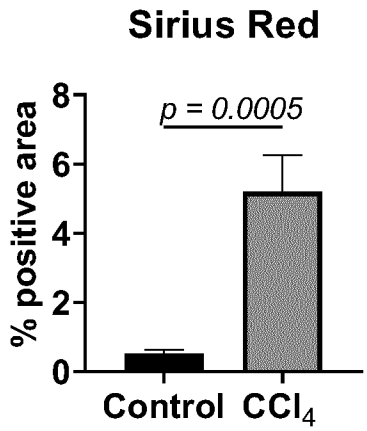
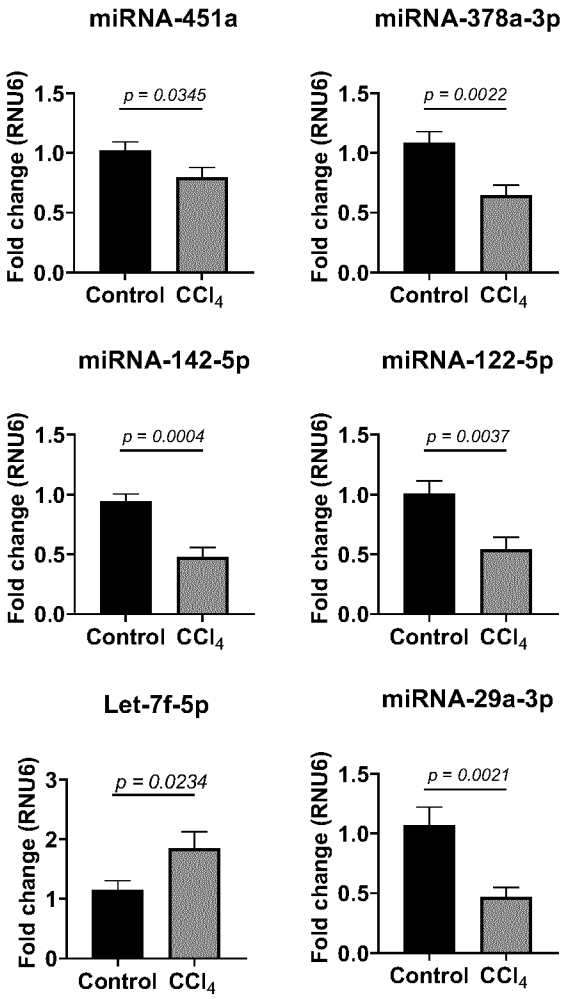

Aff4
Zfp516
Gnai3
Atxn713
Dnajc27
Surf4
Cpeb3
Fold change (Gapdh)
1.5
1.0
0.5
0.0
p = 0.0004
p = 0.0016
p = 0.0003
p = 0.0109
p = 0.0002
p = 0.0059
p = 0.0002
0h
D10

Fig. 8

A


Sirius Red
p = 0.0005
% positive area
0
2
4
6
8
Control
CCl4

B


miRNA-451a
p = 0.0345
miRNA-378a-3p
p = 0.0022
miRNA-142-5p
p = 0.0004
miRNA-122-5p
p = 0.0037
Let-7f-5p
p = 0.0234
miRNA-29a-3p
p = 0.0021
Fold change (RNU6)
Control
CCl4

C

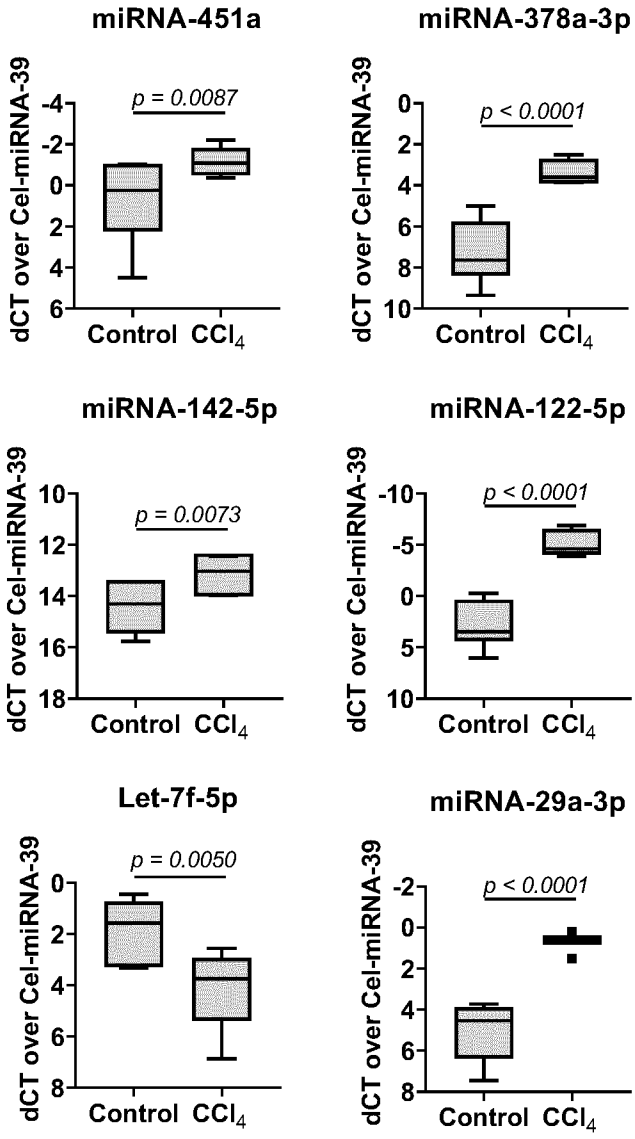

miRNA-451a
p = 0.0087
dCT over Cel-miRNA-39
-4
-2
0
2
4
6
Control
CCl4
miRNA-378a-3p
p < 0.0001
dCT over Cel-miRNA-39
0
2
4
6
8
10
Control
CCl4
miRNA-142-5p
p = 0.0073
dCT over Cel-miRNA-39
10
12
14
16
18
Control
CCl4
miRNA-122-5p
p < 0.0001
dCT over Cel-miRNA-39
-10
-5
0
5
10
Control
CCl4
Let-7f-5p
p = 0.0050
dCT over Cel-miRNA-39
0
2
4
6
8
Control
CCl4
miRNA-29a-3p
p < 0.0001
dCT over Cel-miRNA-39
-2
0
2
4
6
8
Control
CCl4

Fig. 9

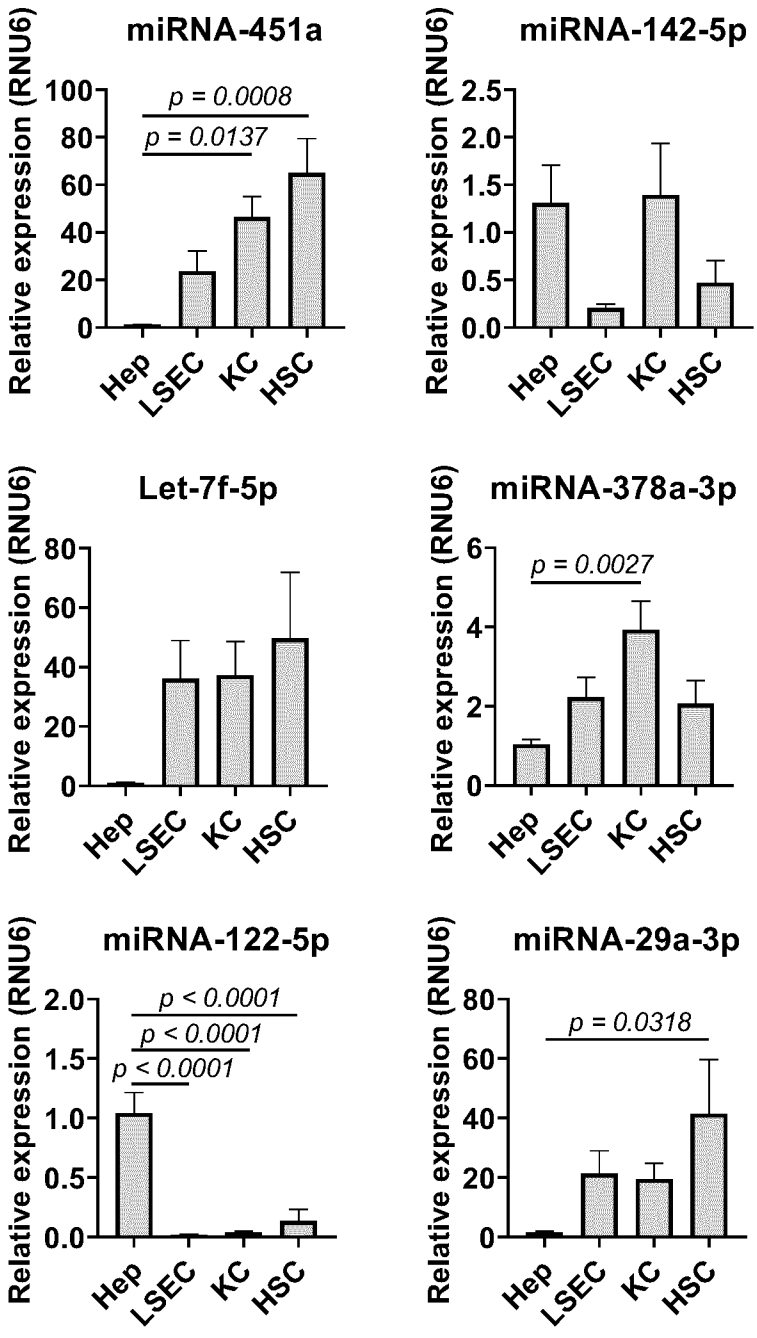
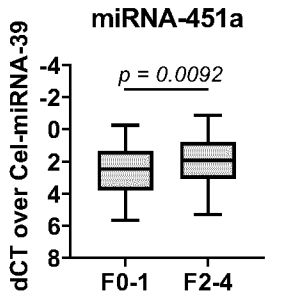
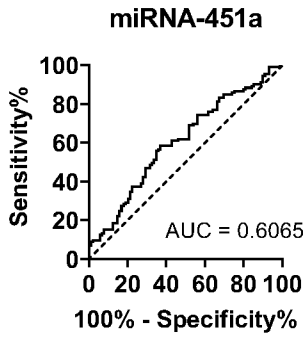
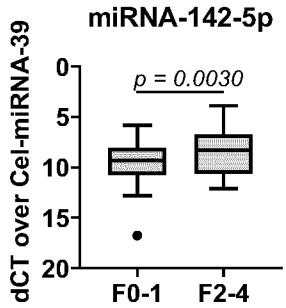

miRNA-451a
Relative expression (RNU6)
p = 0.0008
p = 0.0137
Hep
LSEC
KC
HSC
miRNA-142-5p
Let-7f-5p
miRNA-378a-3p
p = 0.0027
miRNA-122-5p
p < 0.0001
p < 0.0001
p < 0.0001
miRNA-29a-3p
p = 0.0318

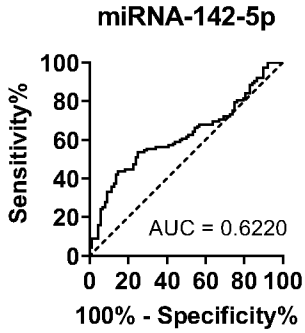
Fig. 10

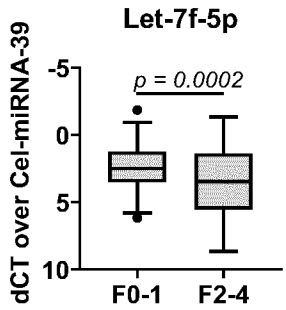
A

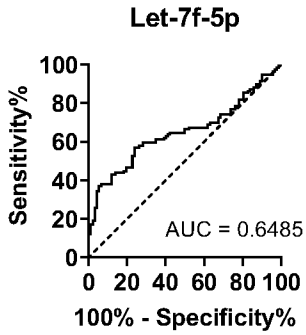

miRNA-451a
dCT over Cel-miRNA-39
p = 0.0092
-4
-2
0
2
4
6
8
F0-1
F2-4

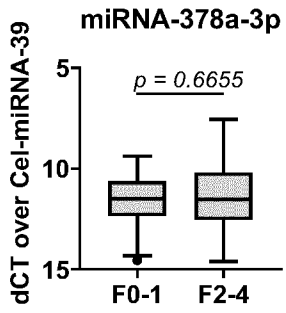

miRNA-451a
Sensitivity%
100
80
60
40
20
0
AUC = 0.6065
0 20 40 60 80 100
100% - Specificity%

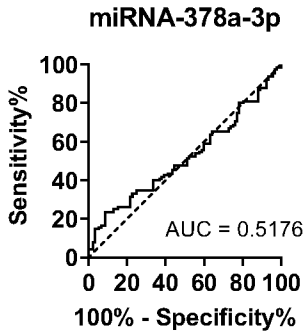

miRNA-142-5p
dCT over Cel-miRNA-39
p = 0.0030
0
5
10
15
20
F0-1
F2-4


miRNA-142-5p
Sensitivity%
100
80
60
40
20
0
AUC = 0.6220
0 20 40 60 80 100
100% - Specificity%

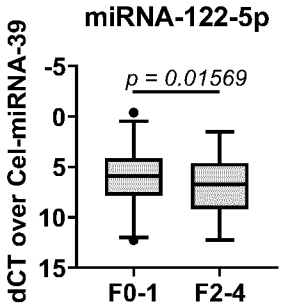

Let-7f-5p
dCT over Cel-miRNA-39
p = 0.0002
-5
0
5
10
F0-1
F2-4

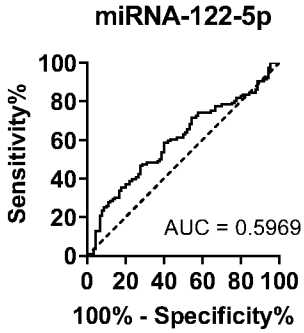

Let-7f-5p
Sensitivity%
100
80
60
40
20
0
AUC = 0.6485
0 20 40 60 80 100
100% - Specificity%


miRNA-378a-3p
dCT over Cel-miRNA-39
p = 0.6655
5
10
15
F0-1
F2-4

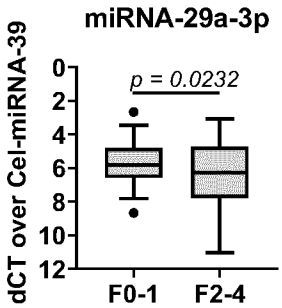

miRNA-378a-3p
Sensitivity%
100
80
60
40
20
0
AUC = 0.5176
0 20 40 60 80 100
100% - Specificity%

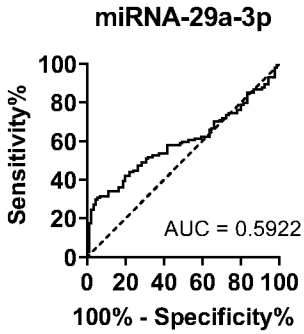
B


miRNA-122-5p
dCT over Cel-miRNA-39
p = 0.01569
-5
0
5
10
15
F0-1
F2-4

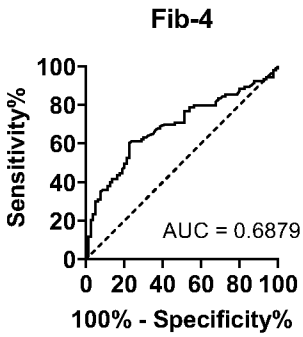

miRNA-122-5p
Sensitivity%
100
80
60
40
20
0
AUC = 0.5969
0 20 40 60 80 100
100% - Specificity%

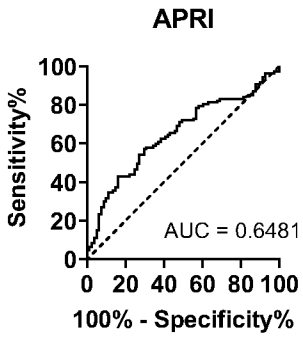
C

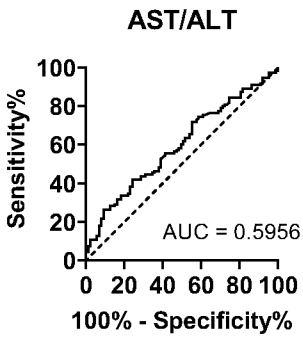

miRNA-29a-3p
dCT over Cel-miRNA-39
p = 0.0232
0
2
4
6
8
10
12
F0-1
F2-4


miRNA-29a-3p
Sensitivity%
100
80
60
40
20
0
AUC = 0.5922
0 20 40 60 80 100
100% - Specificity%

D


Fib-4
Sensitivity%
100
80
60
40
20
0
AUC = 0.6879
0 20 40 60 80 100
100% - Specificity%


APRI
Sensitivity%
100
80
60
40
20
0
AUC = 0.6481
0 20 40 60 80 100
100% - Specificity%


AST/ALT
Sensitivity%
100
80
60
40
20
0
AUC = 0.5956
0 20 40 60 80 100
100% - Specificity%

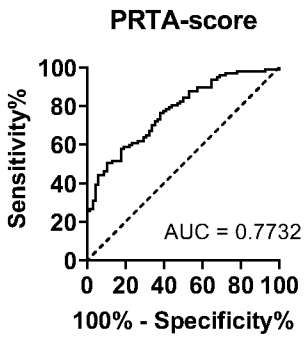

PRTA-score
Sensitivity%
100
80
60
40
20
0
AUC = 0.7732
0 20 40 60 80 100
100% - Specificity%

Fig. 11

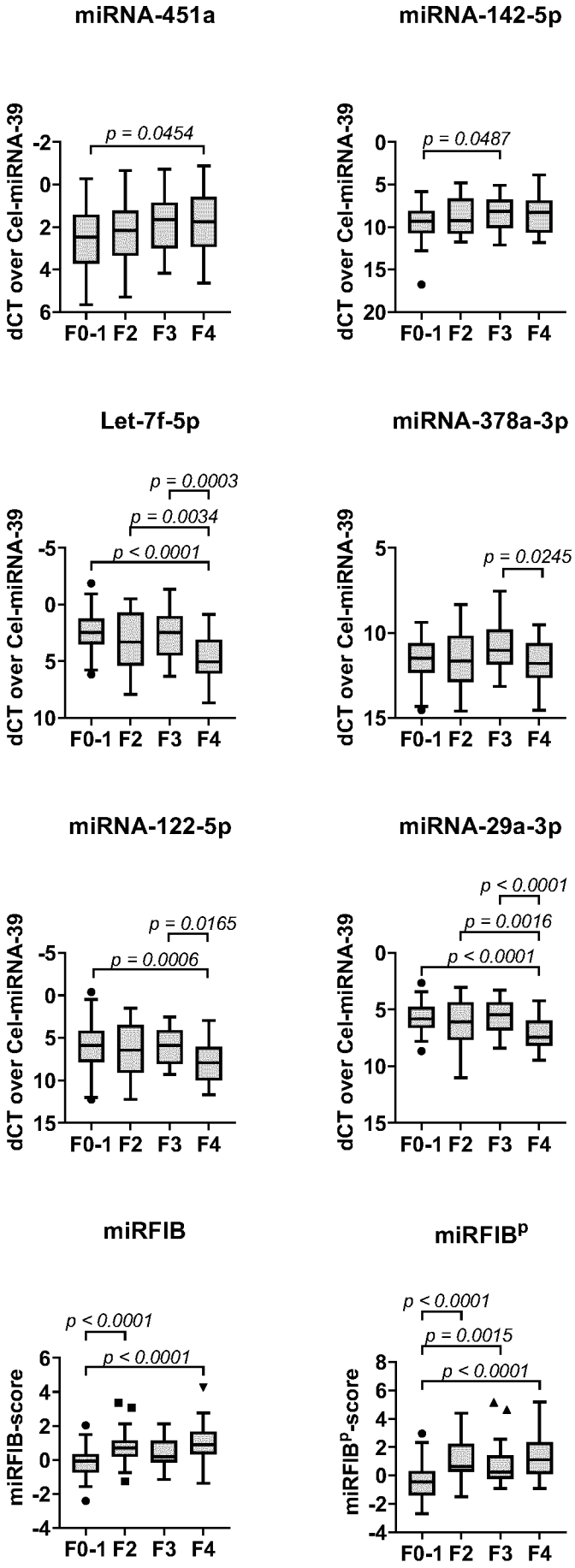
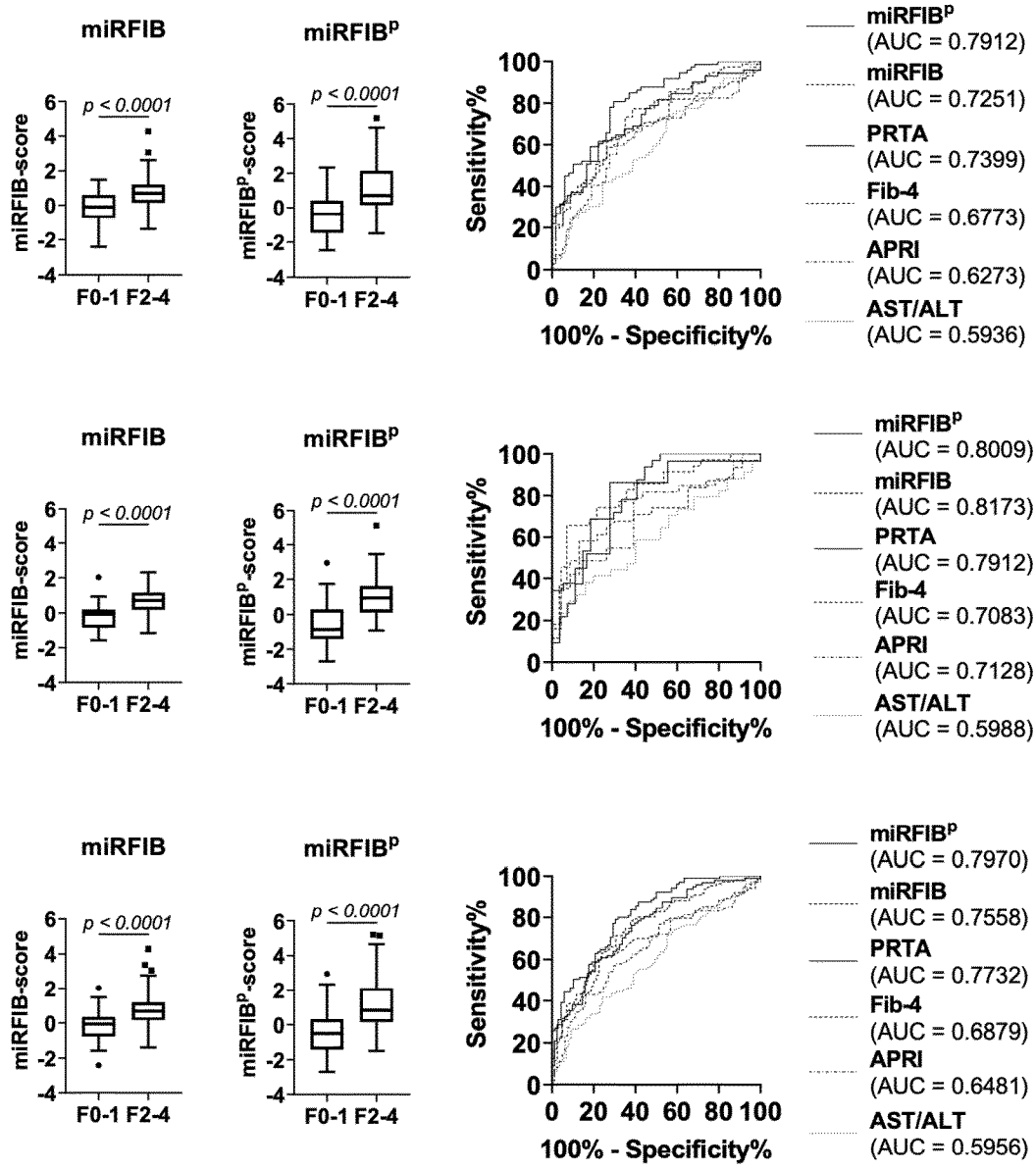

miRNA-451a
p = 0.0454
dCT over Cel-miRNA-39
-2
0
2
4
6
F0-1 F2 F3 F4
miRNA-142-5p
p = 0.0487
dCT over Cel-miRNA-39
0
5
10
15
20
F0-1 F2 F3 F4
Let-7f-5p
p = 0.0003
p = 0.0034
p < 0.0001
dCT over Cel-miRNA-39
-5
0
5
10
F0-1 F2 F3 F4
miRNA-378a-3p
p = 0.0245
dCT over Cel-miRNA-39
5
10
15
F0-1 F2 F3 F4
miRNA-122-5p
p = 0.0165
p = 0.0006
dCT over Cel-miRNA-39
-5
0
5
10
15
F0-1 F2 F3 F4
miRNA-29a-3p
p < 0.0001
p = 0.0016
p < 0.0001
dCT over Cel-miRNA-39
0
5
10
15
F0-1 F2 F3 F4
miRFIB
p < 0.0001
p < 0.0001
miRFIB-score
6
4
2
0
-2
-4
F0-1 F2 F3 F4
miRFIB^p
p < 0.0001
p = 0.0015
p < 0.0001
miRFIB^p-score
8
6
4
2
0
-2
-4
F0-1 F2 F3 F4

Fig. 12


miRFIB
miRFIB-score
p < 0.0001
F0-1 F2-4
miRFIB^p
miRFIB^p-score
p < 0.0001
F0-1 F2-4
Sensitivity%
100% - Specificity%
miRFIB^p (AUC = 0.7912)
miRFIB (AUC = 0.7251)
PRTA (AUC = 0.7399)
Fib-4 (AUC = 0.6773)
APRI (AUC = 0.6273)
AST/ALT (AUC = 0.5936)
miRFIB^p (AUC = 0.8009)
miRFIB (AUC = 0.8173)
PRTA (AUC = 0.7912)
Fib-4 (AUC = 0.7083)
APRI (AUC = 0.7128)
AST/ALT (AUC = 0.5988)
miRFIB^p (AUC = 0.7970)
miRFIB (AUC = 0.7558)
PRTA (AUC = 0.7732)
Fib-4 (AUC = 0.6879)
APRI (AUC = 0.6481)
AST/ALT (AUC = 0.5956)

INTERNATIONAL SEARCH REPORT

International application No
PCT/EP2019/081177

A. CLASSIFICATION OF SUBJECT MATTER
INV. G01N33/68
ADD.

According to International Patent Classification (IPC) or to both national classification and IPC

B. FIELDS SEARCHED

Minimum documentation searched (classification system followed by classification symbols)
G01N

Documentation searched other than minimum documentation to the extent that such documents are included in the fields searched

Electronic data base consulted during the international search (name of data base and, where practicable, search terms used)

EPO-Internal, BIOSIS, CHEM ABS Data, EMBASE, WPI Data

C. DOCUMENTS CONSIDERED TO BE RELEVANT

Category*	Citation of document, with indication, where appropriate, of the relevant passages	Relevant to claim No.
X	WO 2007/021860 A2 (BAYER HEALTHCARE LLC [US]; HAMER PETER J [US]; CARNEY WALTER P [US]; M) 22 February 2007 (2007-02-22)	1-4, 16-20
Y	claims 1-22 page 2, line 19 - line 22 page 3, line 11 - line 15 page 3, line 19 - line 20 page 4, line 2 - line 4 page 5, line 32 - page 6, line 2 page 12, line 15 - line 19	5-15
Y	WO 2015/032414 A2 (UNIV AARHUS [DK]; REGION MIDTJYLLAND [DK]; UNIV SYDNEY [AU]; WESTMEAD) 12 March 2015 (2015-03-12) claim 19 page 52, line 4 - line 11 page 54, line 16 - line 18	5-7,9-12

-/--

[X] Further documents are listed in the continuation of Box C.

[X] See patent family annex.

* Special categories of cited documents :

"A" document defining the general state of the art which is not considered to be of particular relevance

"E" earlier application or patent but published on or after the international filing date

"L" document which may throw doubts on priority claim(s) or which is cited to establish the publication date of another citation or other special reason (as specified)

"O" document referring to an oral disclosure, use, exhibition or other means

"P" document published prior to the international filing date but later than the priority date claimed

"T" later document published after the international filing date or priority date and not in conflict with the application but cited to understand the principle or theory underlying the invention

"X" document of particular relevance; the claimed invention cannot be considered novel or cannot be considered to involve an inventive step when the document is taken alone

"Y" document of particular relevance; the claimed invention cannot be considered to involve an inventive step when the document is combined with one or more other such documents, such combination being obvious to a person skilled in the art

"&" document member of the same patent family

Date of the actual completion of the international search	Date of mailing of the international search report
14 January 2020	04/02/2020

Name and mailing address of the ISA/	Authorized officer
European Patent Office, P.B. 5818 Patentlaan 2 NL - 2280 HV Rijswijk Tel. (+31-70) 340-2040, Fax: (+31-70) 340-3016	Schwachtgen, J

1

Form PCT/ISA/210 (second sheet) (April 2005)

INTERNATIONAL SEARCH REPORT

International application No
PCT/EP2019/081177

C(Continuation). DOCUMENTS CONSIDERED TO BE RELEVANT

Category*	Citation of document, with indication, where appropriate, of the relevant passages	Relevant to claim No.
Y,P	LAMBRECHT ET AL: "The miRFIB-Score: A Serological miRNA-Based Scoring Algorithm for the Diagnosis of Significant Liver Fibrosis", CELLS, vol. 8, no. 9, 29 August 2019 (2019-08-29) , page 1003, XP055657485, CH ISSN: 2073-4409, DOI: 10.3390/cells8091003 abstract paragraph [3.6.] - paragraph [3.7.]	6,8, 12-15
Y	WO 2017/058938 A1 (RES INST AT NATIONWIDE CHILDREN'S HOSPITAL [US] ET AL.) 6 April 2017 (2017-04-06) claims 1-41	6,8,12, 13
A	TIESMAN: "Identification of a soluble receptor for platelet-derived growth factor in cell-conditioned medium and human plasma", JOURNAL OF BIOLOGICAL CHEMISTRY, vol. 268, 5 May 1993 (1993-05-05), pages 9621-9628, XP055535673, US ISSN: 0021-9258 the whole document	1

1

INTERNATIONAL SEARCH REPORT

Information on patent family members

International application No
PCT/EP2019/081177

Patent document cited in search report	Publication date	Patent family member(s)	Publication date
WO 2007021860 A2	22-02-2007	AT 493652 T	15-01-2011
		EP 1913391 A2	23-04-2008
		US 2007037224 A1	15-02-2007
		WO 2007021860 A2	22-02-2007
WO 2015032414 A2	12-03-2015	NONE	
WO 2017058938 A1	06-04-2017	CN 109477144 A	15-03-2019
		EP 3356553 A1	08-08-2018
		US 2018282810 A1	04-10-2018
		WO 2017058938 A1	06-04-2017